Clathrin-mediated post-fusion membrane retrieval influences the exocytic mode of endothelial Weibel-Palade bodies

Nicola L. Stevenson[1,2*], Ian J. White[1*], Jessica J. McCormack[1], Christopher Robinson[3], Daniel F. Cutler[1*‡] and Thomas D. Nightingale[3*‡]

[1]MRC Cell Biology Unit, Laboratory of Molecular Cell Biology, University College London, Gower Street, London, WC1E6BT, UK.

[2]Present address - Cell Biology Laboratories, School of Biochemistry, Medical Sciences Building, University of Bristol, Bristol, BS81TD, UK.

[3]William Harvey Research Institute, Barts and The London School of Medicine and Dentistry, Queen Mary University of London, Charterhouse Square, London EC1M6BQ, UK.

* These authors contributed equally

‡Corresponding authors

Email t.nightingale@qmul.ac.uk

Address: William Harvey Research Institute, Barts and The London School of Medicine and Dentistry, Queen Mary University of London, Charterhouse Square, London. EC1M6BQ, UK.

Phone: +44(20) 7882 8238

 Email d.cutler@ucl.ac.uk

Address: MRC Laboratory for Molecular Cell Biology, Cell Biology Unit and Department of Cell and Developmental Biology, UCL, Gower Street, London. WC1E6BT, UK.

Phone: +44 (20) 7679 7808

Journal of Cell Science • Advance article

JCS Advance Online Article. Posted on 3 July 2017

Summary Statement

Compensatory endocytosis plays key roles in Weibel Palade body exocytosis. Inhibition of this process results in a change of exocytic mode and the release of Von Willebrands factor as tangled strings.

Abstract

Weibel Palade bodies (WPB), the storage organelles of endothelial cells, are essential to normal haemostatic and inflammatory responses. Their major content protein is Von Willebrands factor (VWF) that, following secretagogue-stimulation, is released into the blood vessel lumen as large platelet-catching strings. This exocytosis changes the protein composition of the cell surface and also results in a net increase in the amount of plasma membrane. Compensatory endocytosis is thought to limit changes in cell size and retrieve fusion machinery and other misplaced integral membrane proteins following exocytosis, however little is known about the extent, timing, mechanism and precise function of compensatory endocytosis in endothelial cells. Using biochemical assays, live cell imaging and correlative spinning disk microscopy and transmission electron microscopy assays we provide the first in-depth high-resolution characterisation of this process. We provide a model of compensatory endocytosis based on rapid clathrin and dynamin mediated retrieval. Inhibition of this process results in a change of exocytic mode: WPB then fuse with previously fused WPB rather than the plasma membrane, leading in turn to formation of structurally-impaired tangled VWF strings.

Introduction

Many cell types utilise regulated secretion as a means to release premade bioactive material from membranous carriers at the cell surface[1]. These include soluble factors for release into the extracellular milieu as well as integral membrane proteins that are then displayed for interaction with their cognate ligands. This is absolutely essential for a number of key physiological processes including cell-to-cell communication, immune cell function, digestion, inflammation and haemostasis[1]. The rate and frequency of carrier fusion with the plasma membrane can vary drastically, with the fastest occurring during neurotransmitter release and the slowest during surfactant release from lamellar bodies in pneumocytes[2,3].

Secondary to content release, exocytosis of secretory vesicles causes a net increase in the amount of membrane present at the cell surface. This is particularly apparent in cells with very large granules or cells that undergo rapid release[3-5]. Compensatory endocytosis provides a means to limit this membrane expansion to maintain cell size and membrane tension, as well as to return key integral membrane proteins back into the cell[6,7]. This retrieval process is best understood in neurons and neuroendocrine cells where a number of discrete mechanisms occur. In neurons the mode used depends on the stimulus received and includes full fusion (i.e. collapse) followed by clathrin mediated endocytosis at a separate site, kiss and run exocytosis (whereby a transient fusion event occurs and the granule reseals before collapse), clathrin independent ultrafast endocytosis (UFE) and activity-dependent bulk endocytosis[5,8-10]. During neurotransmission, efficient and sustained neurotransmitter release is absolutely dependent on reformation of synaptic vesicles via clathrin-mediated endocytosis (CME)[6], either directly from the cell surface or from endosomes generated by other endocytic routes[5]. This is a tightly regulated process whereby membrane and specific cargo such as VAMP-2, synaptotagmin-1 and synaptophysin are retrieved in the appropriate ratio to allow reformation of a new synaptic vesicle[5]. During normal physiological stimulation this requires a number of adaptor proteins including AP-2, stonin-2 and AP180[11]. Retrieval in neuroendocrine cells is different; granules do not fully collapse and flatten out at the plasma membrane. Instead they maintain their shape and are re-internalized intact from the plasma membrane in a process referred to as cavicapture[12] or fuse-pinch-linger[13]. These recaptured carriers can then either re-fuse with the plasma membrane at a later stage (if they still contain some cargo) or can be refilled with small transmitter molecules such as amines[4]. This process requires dynamin[12,14,15] and calcium[12] and in some cases allows differential release of cargo based on the size of the fusion pore[4].

The purpose and mechanism of compensatory endocytosis in non-neuronal cell types is poorly characterised, especially in the case of the regulated secretory organelle of endothelial cells, the Weibel Palade body (WPB). WPB contain haemostatic and inflammatory mediators to be released into the vascular lumen[16-18]. The most abundant, and perhaps the most important, WPB cargo is Von Willebrand factor (VWF), a 220kDa glycoprotein that acts as a multifunctional mechanosensitive binding platform for blood components such as platelets. Following synthesis this protein dimerises in the endoplasmic reticulum before transferring to the Golgi. Once in the low pH environment of the trans-Golgi network (TGN) it forms a bouquet structure that stacks into extended coiled tubules. This process, alongside physical constraints imposed by the Golgi apparatus itself[19], confers a unique rod shape and a remarkable length (up to 5μm) to the organelle[18,20]. Furin-mediated cleavage of the pro-peptide and formation of long disulphide-bonded concatemers is also initiated at the TGN and continues during organelle maturation.

Following exocytosis into the pH neutral environment of the blood, and with the help of shear force generated by flow, VWF tubules unfurl and associate to form large platelet-catching strings[21,22]. VWF extrusion is further expedited by some agonists that trigger the formation of a contractile actomyosin ring around the fused WPB membrane[23,24]. Mutations in the VWF gene leading to reduced protein expression, loss of or alterations to its binding sites, or a failure to form concatamers cause Von Willebrand disease, the most common inherited bleeding disorder[18,25]. WPB also contain reservoirs of other proteins such as the type-1 integral membrane protein P-selectin which is trafficked to the plasma membrane to recruit leukocytes in the first step of the leukocyte adhesion cascade[26,27].

To our knowledge few publications have addressed the mechanism of post-exocytic membrane recapture in endothelial cells and none of them in any detail[28,29]. In 2002 Zupancic *et al.* confirmed that full fusion of WPB results in a marked increase in membrane capacitance of 2.5-9.0fF. This is followed by similar size stepwise reductions in membrane capacitance that most likely represent bulk retrieval of membrane[29]. It would therefore appear that at least a proportion of compensatory endocytosis in endothelial cells results from the "en bloc" internalisation of fused exocytic structures. Some, but not all of these events may represent "long lingering kiss" exocytic events where a smaller 12nm pore forms and eventually reseals following WPB fusion. This is thought to be the case for 10% of exocytic events during strong stimulation[30]. Clathrin-coated pits, which may represent compensatory endocytic structures have also been noted on large secretory pod-like

structures which are thought to result from intracellular fusion of WPB[28]. Whether these form before or after WPB fusion with the plasma membrane is unresolved[28,31].

It is unclear whether compensatory endocytosis in endothelial cells serves a purpose beyond retrieval of membrane. WPB by necessity must form at the TGN to allow normal release of functional strings[32,33]; once exposed to pH 7.4 and unfurled, the VWF cannot be refolded. Compensatory endocytosis following VWF release thus cannot lead to the regeneration of functional granules for re-use as in neuroendocrine or neuronal cells[6]. It is also unlikely to be required for retrieval of known integral membrane cargoes such as P-selectin and CD63 as these rapidly diffuse away from the WPB fusion site and can be retrieved through general endocytic pathways[34,35]. Finally if the purpose of WPB compensatory endocytosis is solely to retrieve membrane then this could be carried out anywhere on the plasma membrane and begs the question, why have clathrin-coated pits been noted on VWF containing fused-structures?

To address these issues, we investigated this process in human umbilical cord endothelial cells (HUVEC) using biochemical assays, transmission electron microscopy (TEM) and correlative live cell imaging and TEM to define the extent, mode, mechanism and function of compensatory endocytosis. We demonstrate that changes in compensatory endocytosis affect the exocytic mode of WPB.

Results

A biochemical assay for monitoring compensatory endocytosis

Generally throughout this study we use PMA as the stimulus for exocytosis for a number of reasons. Firstly, there are a large number of secretagogues that stimulate WPB exocytosis (more than 30) some of which trigger a Ca2+ dependent release and some of which act via cAMP[36] and PMA uses both: we wanted to monitor the effect on endocytosis irrespective of the route of stimulation. Indeed during physiological stimulation endothelial cells are likely to be stimulated by multiple secretagogues at once and this often has a synergistic effect on release[37]. Secondly, later in this study we use a number of approaches to limit content release and endocytosis and as such it is important to use a secretagogue that will be unperturbed by such manipulations. As PMA is a lipid it doesn't require cell surface receptor binding for its action. Therefore when we analyse results we can exclude effects of pH on receptor ligand binding (e.g. Histamine activates endothelial cells less efficiently at low pH[35]), similarly we can exclude effects due to changes in receptor down regulation (as might occur during inhibition of endocytosis). Thirdly, PMA provides a strong stimulation and this

makes monitoring its effect on endocytosis by biochemical or electron microscopy approaches as unequivocal as possible.

To characterise the extent of compensatory endocytosis in endothelial cells we began by comparing the rate of incorporation of fluid phase markers into unstimulated and phorbol 12-myristate 13-acetate (PMA) stimulated HUVEC. An assay monitoring horse-radish peroxidase (HRP) uptake provided the most robust data. This is likely because even small amounts of HRP can be detected with great sensitivity using the Tyramide Signal Amplification (TSA) system. After 15 minutes of uptake, HRP can be found generally in early endocytic organelles as shown by partial co-localisation with EEA-1, an early endosomal marker (Fig. 1A). Similarly transferrin internalised for 2 min and then chased for 15 min parallels the endocytic trafficking of the HRP (Fig. 1B). To show that HRP internalisation follows the fate of WPB components after exocytosis, we looked at its co-localisation with P-selectin, a WPB cargo. In unstimulated cells, P-selectin localised to rod-shaped structures throughout the cytosol and did not exhibit any significant co-localisation with HRP. However, following PMA stimulation, P-selectin appeared in small surface patches as well as in intracellular punctate structures which frequently, but not always, co-localised with HRP and were therefore endocytic (Fig. 1C) (Table S1). Importantly, treating HUVEC with PMA or a cocktail of Histamine and adrenaline for 15 minutes to stimulate WPB exocytosis resulted in a significant and reproducible increase in the amount of internalised HRP (Fig. 1D, Fig. S1A) suggesting endocytosis was upregulated. To determine the proportion of this increase that was dependent on the exocytosis of WPB, and to confirm that it was not an off-target effect of the secretagogue treatment, we knocked down (kd) VWF and measured HRP uptake in depleted cells. Post kd cells lack VWF (Fig. 1E) and recognisable WPB and show negligible increase in HRP incorporation following stimulation compared to controls (Fig. 1D). From this we can conclude that almost a third of HRP incorporation post stimulation labels compensatory endocytic structures.

We did attempt to use live cell imaging to monitor compensatory uptake in real time by following the incorporation of lipophilic dyes FM1-43 and FM4-64 into fused WPB (as denoted by the loss of GFP-tagged VWF). This proved difficult to characterise and quantify due to the high background noted both with spinning disk and point scanning confocal microscopy. Functional exocytic events (that release VWF strings into the blood flow) occur at the apical surface and this precluded our use of approaches such as TIRF microscopy. We did have some limited success by assaying the incorporation of 10kDa dextran-tetramethylrhodamine into fully fused WPB live, but again it was difficult to use this approach robustly as it labelled such vast numbers of structures with such a high

background of fluorescence that quantification was inconsistent. Preliminary evidence from this work did, however, indicate that fusion of the WPB at the cell surface creates a compartment open to fluid phase markers, which at least in the few instances we characterised, do not collapse into the membrane during the time of imaging (Fig. S1B)

Ultrastructural time-resolved analysis of compensatory endocytosis

To characterise the route of compensatory endocytosis, as well as the timing and localisation of such events, we exploited a previously published assay to monitor the ultrastructure of exocytic sites in a time-resolved manner[24]. We co-transfected endothelial cells with a GFP-tagged version of VWF and a truncated version of P-selectin lacking the transmembrane domain and cytoplasmic tail (mCherry-PselectinLum). The former construct allows monitoring of VWF content release while the latter allows precise timing of the point of WPB fusion as it diffuses away rapidly in the medium[24]. Cells were plated on gridded coverslip-bottomed dishes to allow precise localisation in x and y (Fig. 2A-D). Following stimulation with PMA we imaged transfected cells using high speed spinning disk confocal microscopy and added fix at arbitrary time points (Fig. 2E). We then correlated the light microscopy with an EM analysis (correlated light and electron microscopy-CLEM) using serial sections. By monitoring the loss of mCherry-PselectinLum we could precisely define how long from the point of fusion each exocytic event was fixed and thus correlate any compensatory endocytic structures seen by EM with time post fusion (Fig. 2Eii). All events characterised by this approach are full fusion events as the mcherry-PselectinLum construct is too big to be released by the 12nm pore reported as present during lingering kiss fusion[30].

In total we carried out such analyses in six separate experiments. Compensatory events (defined as endocytic budding profiles present on fused WPB) were first seen 20 seconds after fusion, and fully invaginated endosomes were apparent as early as 30 seconds post fusion (Fig. 3). These early retrieval events took place whilst the exocytic pore was open and continued at later time points (60-75s) as the pore closed. All events examined were clathrin-coated and occurred directly on the exocytic structure. The compensatory endocytic structures also often contained electron dense material that in most cases appeared to be near the membrane of the vesicle (Fig. 3). Fully fused WPB contained some VWF and there were apparent attachment sites between the internal VWF and the exocytic membrane. Note, endocytic events were not present on all exocytic structures (we quantified this more fully in fixed CLEM experiments Fig. 5 & 6).

These results indicate that retrieval of WPB membrane, and presumably membrane proteins, begins very soon after fusion, and can occur while a pore (which can last over a minute) is open. Capacitance data indicates that, at least in some cases, the whole WPB membrane is retrieved intact from the plasma membrane after fusion[29]. This combined with our ultrastructural data suggests a model whereby there is some immediate retrieval following WPB fusion, then the plasma membrane reseals and the internalised vacuolar structure is further "nibbled" by smaller clathrin-coated buds to retrieve yet more membrane and integral membrane proteins.

Low pH prevents unfurling of VWF

The large stepwise decrements recorded by capacitance analysis suggest pore sealing and bulk retrieval of WPB membrane is a general consequence of exocytosis of these huge granules[29]. This should be sufficient to maintain cell size homeostasis yet we observed a number of retrieval events that occur before pore closure (Fig. 3). This strongly suggests there is an urgent requirement for the removal of membrane content introduced by exocytosis from the cell surface. To determine the relationship between pore closure and retrieval we sought ways to limit the former by preventing the unfurling of VWF into strings. One way to do this is by minimising the pH change associated with exocytosis. When release of VWF occurs at lower pH, such as might occur during acidosis (pH 6.5), the rate of VWF unfurling is significantly slower and thus its release through the pore is delayed, blocking closure[35]. The internal pH of WPB is 5.5[22]. We therefore reduced the pH in the bathing medium of HUVEC to mirror this and stimulated exocytosis using PMA before labelling external and total VWF. At neutral pH we saw collapsed WPB releasing VWF as pronounced strings as well as rod-shaped WPB that are yet to fuse with the membrane (Fig. 4A). At pH 5.5 most of the WPB remained rod-shaped (we did see some collapsed or more rounded WPB but they were markedly less common) and no strings of VWF were seen (Fig. 4B). We also monitored fusion using live cell imaging. At pH 7.4 we noted a rapid loss of mCherry-PselectinLum and a transient increase in GFP-VWF intensity, followed by a more gradual diffusion away of the content as expected (Fig. 4C). During exocytosis at pH 5.5, however, mCherry-PselectinLum exits more slowly and the GFP-VWF signal initially increases then remains largely the same for extended periods (Fig. 4D).

VWF content release is required for normal compensatory endocytosis and WPB fusion

To determine what happened to compensatory endocytosis at these unresolved fusion pores, we carried out CLEM of PMA-stimulated cells undergoing exocytosis at pH 7.4 (Fig. 5A & C) and at pH 5.5 (Fig. 5B, D-G). Following fixation we labelled external VWF with 10nm gold to demonstrate conclusively that VWF had been exocytosed and carried out serial sectioning. As we and others have

previously found[22,24,38], at pH 7.4 collapse of the WPB from a rod- to a round-shaped structure is apparent, as is the release of VWF as strings (Fig. 5A & C). Fusion at pH 5.5 results in varying degrees of collapse from structures that remain almost entirely rod-shaped (Fig. 5D), to slightly swollen fused structures (Fig. 5F) and WPB that have actually collapsed (Fig. 5E). In all instances, at pH 5.5 we saw much more highly structured VWF that also showed some filamentous attachment to the organelle membrane.

When we quantified the number of compensatory endocytic structures on fused WPB under each condition we noted an increase in events at lower pH (Fig. 5H). At pH 7.4, 25% of events seen by CLEM have compensatory profiles (between 1 and 3) whilst the remaining 75% lack obvious structures. In contrast, 70% of fused structures have up to 5 compensatory events at pH 5.5. This could indicate that either compensatory structures are taking longer to resolve at pH 5.5 or that more endocytic events are occurring.

Importantly, we also saw a change in the exocytic mode at pH 5.5, namely a marked increase in what appeared to be cumulative exocytosis whereby a fused WPB acts as an exocytic site for a second such organelle. In some situations we saw up to four WPB in close apposition with each other, such that their membranes are touching (Fig. 5G). Such apparent cumulative fusion was a relatively rare occurrence under control conditions with only 10% of fusing WPB exhibiting some membrane to membrane contact with another WPB. In contrast, following a reduction in the pH of the bathing medium this increased to more than 50% of events (Fig. 5I).

WPB exocytic mode is influenced by VWF content release

To determine if the change in exocytic mode and the number of compensatory endocytic profiles was due to a failure to unfurl VWF tubules at low pH or a more general effect of delaying content release we identified other approaches to inhibit the latter. We have previously demonstrated that an actomyosin ring is required for efficient expulsion of VWF following PMA stimulation[24]. Inhibition of this mechanism can thus be used to prevent resolution of fusion at normal pH. Under control conditions, VWF was released from the fused WPB and projected as strings above the plasma membrane in serial EM sections (Fig. 6A). However, in conditions where actin polymerisation was inhibited using cytochalasin E (CCE), we saw fused structures with pieces of membrane still covering parts of the open pore (Fig. 6B). We have previously shown that these structures can persist for over 300s[24]. When we analysed the number of compensatory vesicles present on these fused WPB we saw only a small increase following CCE treatment (Fig. 6E). This had no effect on the rate of

cumulative fusion (Fig. 6F). In fact in some CCE treated cells we saw multiple exit sites occurring in very close proximity with no evidence of cumulative fusion (Fig. S2). This demonstrates that the presence of a fused structure alone does not affect the exocytic mode.

As a third alternative approach to prevent VWF unfurling, we stimulated cells in the presence of an anti-VWF antibody in the bathing medium. Under these conditions we noted an arrest of VWF near the exocytic site (as has been published previously[39]) and no strings were formed. This method had a greater effect on the number of compensatory structures seen than CCE and a minor effect on cumulative fusion (Fig 6C, E & F). The most marked effects were apparent when we combined the anti-VWF antibody and CCE (Fig. 6D). Here we noted multiple compensatory endocytic profiles on almost all events (90%) (Fig. 6E) and a marked increase in cumulative fusion, similar to the effects of low pH (Fig. 6F). Generally, therefore, we noted a correlation between the number of compensatory endocytic structures and cumulative exocytosis. There was a threshold effect, with marked amounts of cumulative fusion only occurring when more than 70% of events had compensatory structures. This demonstrates that cumulative fusion is increased in situations where VWF cannot fully exit the cell and the pore is prevented from closing normally.

Compensatory endocytosis is required for normal WPB fusion

The increase in frequency with which we observe compensatory structures by EM could be due to an increase in the number of events occurring or in the time it takes to resolve the structure and complete scission. To address this question we interfered with the endocytic process directly. We know that compensatory endocytic events require clathrin from our electron microscopy experiments (Fig. 2 & 3) and we could also see clathrin co-localising with the sites of VWF exocytosis (Fig. S3). We therefore chose to target this molecular aspect of the endocytic process. Blocking clathrin function on a long-term basis interferes with constitutive endocytosis and the formation of WPB[32], so we used the dynamin inhibitor dynasore[40]. To corroborate the effects of this treatment we also knocked down (kd) the likely adaptor protein AP-2 (by transfecting siRNA targeting the alpha subunit[41,42]). Dynamin is required for both clathrin-dependent and some clathrin-independent pathways and is necessary for fluid phase HRP uptake[15] whereas AP-2 is required solely for clathrin mediated endocytosis[41,42]. Dynasore allows an acute inhibition of this process whereas siRNA treatment required 3 or 4 days. AP-2 alpha kd cells had on average 74% the levels found in mock-treated cells by western blot (Fig S4A & B). We did see some co-localisation of dynamin II and external VWF by confocal microscopy but perhaps due to the transient nature of dynamin function such events were relatively rare (Fig. S3).

Treatment of HUVEC with 25µM dynasore or AP-2 alpha siRNA blocked transferrin uptake as expected (Fig. 7C) and in the case of dynamin treatment caused a marked change in the exocytic mode as revealed by electron microscopy (Fig. 7A & B). We often noted chains of large mostly empty vacuoles in close apposition, stretching from the plasma membrane into the cytoplasm. These often contained some remnants of VWF cargo. We also noted the presence of unfused WPB touching some of these vacuoles (Fig. 7A & B). As expected many more clathrin-coated endocytic profiles were apparent and these often exhibited wide necks, presumably due to the inhibited pinch-ase function of dynamin (Fig. 7B). Definition and therefore accurate quantification of exactly which vacuoles unambiguously represented previously fused WPB was difficult as not all such vacuoles contained obvious VWF content (previous analysis was possible due to arrested VWF secretion or by using gold conjugated anti-VWF labelling at the cell surface). To corroborate the electron microscopy we also carried out live cell imaging of the exocytosis of WPB labelled with VWF-GFP in the presence or absence of 25µM dynasore or following treatment with siRNA targeting the AP-2 alpha subunit. In control cells WPB fused in close proximity without merging (Fig. 7D & E). Following dynasore treatment (Fig. 7D & F) or AP-2 alpha siRNA treatment (Fig. 7D & G) a greater proportion of exocytic events merged into one another suggesting cumulative fusion. Dynasore treatment did not affect the rate of granule collapse or the extent of lingering kiss fusion. The difference in cumulative fusion quantified by live cell imaging although significant is lower than from EM quantification. This is likely due to an underestimation of cumulative fusion events due to the release of VWF-GFP (it is impossible to tell if fused structures merge if the content has already been released from one of these structures). This data supports the conclusion that the increase in cumulative exocytosis shown by blocking content release is due to an inhibition of compensatory endocytosis.

Cumulative fusion of WPB results in improper release of VWF strings

To investigate whether the switch toward cumulative fusion would have functional consequences, we analysed the release of VWF and the formation of platelet-catching VWF strings under different conditions. Live cell imaging indicated no difference in the number of WPB fusions events per cell following dynamin inhibition (Fig. 8A), yet we noted a small but significant decrease in the amount of VWF secreted (approximately 29.2%+/-2.4, Fig. 8B). The depletion of AP-2 alpha by siRNA resulted in a similar reduction in the fraction of total cellular VWF released (approximately 21.15%+/-4.0, Fig. 8B), yet an overall increase in the number of fusion events. Further analysis revealed this was due to a significant increase in WPB number (Fig. S4C) and VWF levels (Fig. S4D & E) in AP-2 kd cells. This

most likely reflects a long term-effect of AP-2 depletion (see discussion below). Despite this increase in WPB number we still see the same effects on cumulative fusion and the fraction of VWF released.

The analysis of VWF string number and length under flow demonstrated that there was a marked reduction (more than 2 fold) on the number of strings/cell following dynasore treatment (Fig. 8C) with little overall effect on string length (Fig. 8D) (apart from perhaps for very long VWF strings). This indicates that cumulative exocytosis results in aberrant release of VWF, most probably due to its inefficient release as tangled strings. Interpretation of the effect of the longer term AP-2 kd on string length was impossible due to the increase in WPB number relative to the mock transfected control (Fig S4C-E), so that we were unable to separate the effects on string length of tangled VWF from the effects on WPB number.

Discussion

The work described here demonstrates that compensatory endocytosis in endothelial cells is a major endocytic route and is likely to significantly influence a normal haemostatic response. By measuring the incorporation of fluid phase HRP in the presence or absence of WPB we have determined that approximately one third of endocytic uptake by volume – as measured by HRP uptake - following PMA stimulation is internalised by compensatory pathways (Fig. 1). Essentially all of this stimulated endocytosis was due to WPB exocytosis, with a minimal contribution via fusion of other organelles such as lysosomes. We also provide the first ultrastructural characterisation of compensatory endocytosis in endothelial cells. We show that the majority of WPB exocytic events, not just the minority comprising lingering-kiss (endothelial kiss and run[30]) events, do not result in full fusion i.e. total collapse of the organelle into the plasma membrane (Fig. 2, 3). Instead, fused empty WPB persist as distinct structures on which clathrin-coated budding vesicles assemble as early as 20 seconds post exocytosis. The formation of clathrin-coated vesicles occurs irrespective of whether the pore is open and they often contain membrane associated electron dense cargo. Fusion pores close after approximately 60-75s whilst clathrin-mediated budding continues. This model of retrieval is in line with the cavicapture events seen in chromaffin cells[4,43], i.e. recapture of the profile followed by continued CME "nibbling" to break down the structure. Such a model agrees with published analysis of capacitance changes during regulated release in endothelial cells[29]. Over extended measurements, symmetrical distribution of positive (exocytic) and negative (endocytic) event amplitudes have been characterised indicating that a similar amount of membrane is added to the plasma membrane as is retrieved. The proportion of events resolved between 0.5-110fF account for

approximately 33% of the capacitance change and this is in line with the changes we note in HRP uptake on PMA stimulation. Our ultra-structural approaches only monitor events that occur directly on the exocytic structure and we are only addressing one stimulus. As such we can't rule out the presence of additional compensatory endocytosis at discrete sites including events such as ultrafast endocytosis and activity dependent bulk endocytosis[5] in this study. Given that the rate of WPB fusion (relative to synaptic vesicle release) is relatively slow and the exocytic capacitance changes approximately mirror endocytic changes their contributions are likely to be relatively minor.

We didn't note any clathrin coated pits on mature WPB (typified by electron dense tubules of VWF) or on fusion events earlier than 20s post fusion. Indicating such events occur post exocytosis. Clathrin coated buds have been noted on immature (electron lucent) WPB near the TGN, presumably reflecting the retrieval of mis-sorted granule components[44].

The function of compensatory endocytosis in endothelial cells is likely to be very different from other systems, such as in neurons, where the primary purpose is to quickly replenish synaptic vesicles to maintain exocytic output. Functional WPB can only be formed at the TGN[16,32,44,45] thus any direct replenishment by compensatory endocytosis would be impossible. Also we have shown that direct inhibition of endocytosis using dynamin inhibitors had little effect on the extent of WPB fusion (Fig. 8A). Despite this, the assembly of clathrin-coated structures directly on the WPB membrane so soon after fusion does suggest a requirement for rapid retrieval of certain proteins or lipids (Fig. 3). Our data suggest a link between content release, compensatory endocytosis and exocytic mode. We manipulated conditions to drive incomplete VWF release, using either bathing medium at low pH, the presence of anti-cargo antibody in the bathing medium, or inhibition of actin remodelling. These treatments all resulted in an increased number of compensatory profiles. All of these approaches have their own particular limitations (more gross effects of the pH change, global effects on the cytoskeleton etc.) but despite these differing limitations the same consensus effect is apparent i.e. a change in exocytic mode is coupled to a change in clathrin coated structures. This change in exocytic mode is also phenocopied by more specific approaches; the acute inhibition of endocytosis using the dynamin inhibitor dynasore or the longer term siRNA mediated depletion of Ap-2 alpha, together indicating this is an endocytosis specific phenomenon (Fig. 7).

Importantly, the changes in content release that drive the increase in compensatory structures also produced a change in exocytic mode, with cumulative fusion events becoming markedly more common. We noted a correlation between the number of compensatory structures seen and the

incidence of cumulative fusion (Fig. 5 & 6); the greatest effects on cumulative exocytosis occurred when compensatory structures were present on more than 70% of events. This suggests there may be some sort of threshold effect involved. It is unclear precisely how inhibition of VWF content release influences compensatory endocytosis. Perhaps this is simply a physical constraint due to difficulty retrieving membrane from a structure still containing content or perhaps resealing of the granule is necessary for efficient endocytosis. Alternatively, it might be that signalling events are triggered following content clearance that acts upon the endocytic machinery. We also noted an increase in the total amount of VWF within AP-2 alpha kd cells by western blot (Fig. S4D) and ELISA (Fig. S4E). The reasons for this increase are unclear. Clathrin and AP-1 are required for WPB formation[32] and long-term inhibition of Ap-2 may therefore result in increased pools of unused clathrin and consequently an increase in WPB number. Alternatively inhibition of AP-2 might have interfered with a signal required to limit WPB formation or control the basal release of WPB.

Our data indicates the change in exocytic mode is due to compensatory events that are arrested, or resolve more slowly. We propose that this affects exocytosis by causing a failure to release for re-distribution membrane proteins required for exocytosis (see model Fig. 8E). This leads to an accumulation of the fusion machinery and associated components at sites that then drives cumulative exocytosis. In neurons compensatory endocytosis has been shown to play a role in clearing exocytic machinery from release sites[5,46,47]. We hypothesise that this is also the purpose of the early clathrin-mediated events on fused WPB membranes. Failure to resolve compensatory endocytic events increases cumulative fusion to over 50% (from TEM characterisation) (Fig. 4-7). We have yet to determine the integral membrane proteins that are retrieved from WPB (this research is in progress). During neurotransmission, the molecules retrieved include vSNAREs, synaptotagmin and synaptophysin[5]. In endothelial cells the only analogous characterised membrane bound machinery shown to be localised to WPB are the v-SNARES VAMP-3 and -8[48]. Interestingly, sequential fusion of granules in pancreatic acinar cells has shown to be dependent on the retrieval of VAMP-8. Mice lacking this SNARE exhibit a specific reduction in secondary fusion events (granule to granule) with no difference in the fusion of granules with the plasma membrane[49]. Other factors that are likely to play a role in the amount of cumulative fusion are the number of WPB and the rate of exocytosis. Live cell imaging of WPB exocytosis following dynamin inhibition demonstrated cumulative exocytosis was most common when the fusion rate was high.

Control of the exocytic mode is important to allow the release of a normal complement of VWF strings under flow (Fig. 8). Acute inhibition of compensatory endocytosis does not affect the extent

of WPB fusion (Fig. 8A) but does result in a small inhibition of VWF release (Fig. 8B). However, the effect on the number of VWF strings is much more marked. (Fig. 8C) indicating that cumulative fusion is significantly less effective for releasing strings of VWF under flow. This mode of release results in a greater amount of VWF being released through one pore, the strings are therefore much more likely to be tangled and the shear force would presumably less efficiently act to pull strings out at the cell surface. This is likely to have a negative effect on platelet recruitment, and thus haemostatic function.

Generally, and in various cell types, two different mechanisms of bulk exocytosis can occur[50]. In mast cells compound exocytosis results from granules fusing with each other before fusing with the plasma membrane[51] whereas during cumulative exocytosis, as occurs in the pancreatic acinar, granules fuse with others that have already exocytosed. Both mechanisms allow for focussed content release at a very small plasma membrane region[52,53]. Our experiments at low pH strongly suggest a cumulative rather than a compound mode of content release for WPB. The WPB are more rod-shaped at low pH even after fusion and we can tell that this fusion is sequential as the most collapsed structure is always adjacent to the plasma membrane and the WPBs fusing with this become progressively more rod-shaped deeper within the cell. Cumulative fusion events in endothelial cells have been suggested to occur previously by monitoring the transfer of overexpressed CD63-GFP from sequentially fusing WPB[54], but such events have never been previously characterised at the TEM level nor quantified. Compound exocytosis has also been reported to occur in endothelial cells by the formation of a pre-fusion structure termed a secretory pod[28]. This is thought to form by fusion of WPB with each other before subsequent fusion with the cell surface. Interestingly these structures also exhibit apparent compensatory structures. If such a model is correct it would require a pH change as the WPB that form the pod are collapsed and contain disordered VWF. As to how this occurs is as yet unresolved. Capacitance analysis of WPB undergoing stimulation does to some extent support compound exocytosis, as steps which represent more than a single WPB have been noted, although infrequently[29]. In our experiments we noted that the presence of antibody in the bathing medium alters exocytic mode. Given that the initial characterisation of the secretory pod was carried out in medium with anti-VWF antibody to capture and label exocytic sites, we suggest that this will likely have affected the interpretation of the results[28]. An alternate model for pod formation supported by our data would be cumulative fusion of WPB with resealed lingering kiss structures. This would result in large internal structures and, due to the frustrated nature of VWF release, these would also be decorated with more compensatory

endocytic structures. The authors of the paper describing secretory pods highlight the possibility of this model in a more recent publication[31].

We also noted attachment of VWF to the sides of exocytic structures. This has been seen before[28] and its purpose is as yet unclear. VWF attachment occurs at both pH 5.5 and pH 7.4 suggesting that it is present before the tubules unfurl and the granule collapses. It may therefore represent a means to anchor strings to support orderly unravelling of content. Interestingly, in immature WPB the VWF tubules are clearly spaced away from each other and especially from the membrane along the organelles longitudinal axis, whereas inter-tubule structures can occasionally be seen, and the tubules appear to touch the limiting membrane at the organelles tips. Whether the attachment sites of VWF content to the fused structure involves the same elements is not yet clear.

Overall we provide the first characterisation of compensatory endocytosis in endothelial cells using biochemical and novel ultrastructural techniques. By fully characterising this pathway, we were able to demonstrate that it influences the exocytic mode of WPB. This is a novel function for this poorly understood process in endothelial cells, and is particularly important for VWF exocytosis whereby orderly release of untangled VWF strings is a prerequisite for effective platelet recruitment and thus haemostasis.

Materials and Methods

Cell culture and transfection

Human Umbilical Vein Endothelial Cells (HUVEC, promocell, Heidelberg, Germany) were cultured as previously described[33]. Plasmid transfections were performed by nucleofection (Nucleofector II, programme U-001, Amaxa Biosystems, Gaithersburg, MD) using 2-5μg DNA. GFP-VWF[55] was a gift from J. Voorberg and A. Van Mourik (Sanquin Research Laboratory, Amsterdam, Netherlands). The synthesis of C-terminal–tagged mCherry-PselectinLum fusion construct was described in Nightingale *et. al.* 2011[24]. Mock, VWF and Ap-2 alpha siRNA transfections were performed as in Ferraro *et. al.* 2014[19] using firefly luciferase siRNA 5'-CGUACGCGGAAUACUUCG-3', VWF siRNA 5' GGGCUCGAGUGUACCAAAATT 3' and AP-2 alpha siRNA 5'AAGAGCAUGUGCACGCUGGCCA[41] (Qiagen, Hilden, Germany).

Antibodies and reagents for immunofluorescence

Rabbit anti-VWF was purchased from DAKO, Ely, UK. Sheep anti-VWF and sheep anti-TGN46 were purchased from BIORAD, Oxford, UK. Sheep polyclonal anti-P-selectin was from R&D systems,

Abingdon, UK, mouse monoclonal anti-EEA1 (clone 14) and mouse anti-adaptin alpha was from BD Pharmingen, Oxford, UK and mouse anti-clathrin light chain (CON.1) and mouse anti-tubulin were from Sigma, Gillingham, UK.

HRP assays

HUVEC were incubated with 1mg/ml HRP (Sigma, Dorset, UK) +/- 100ng/ml phorbol 12-myristate 13-acetate (PMA) for 15 minutes at 37°C, then washed thoroughly on ice and fixed in 4% formaldehyde (PFA, Polysciences, Edenkoben, Germany). HRP was visualized by fluorescein-tagged tyramide signal amplification; TSA-fluorescein (Perkin-Elmer, Beaconsfield, UK) was diluted 1:150 in the provided diluent and incubated with coverslips for 2 minutes before stopping the reaction with a 30 second incubation with 0.2% (w/v) sodium azide. Cells were then washed with PBS, antibody labelled and imaged as above. For co-localisation with transferrin, 20µg/ml Alexa Fluor 568-conjugated transferrin (Life Technologies, Paisley, UK) was included in the incubation medium. For quantification, 10 fields of view were taken at random per experiment and HRP positive objects quantified using Image J software; background subtraction was performed using a rolling ball algorithm (2 pixels) and a threshold manually applied prior to performing particle analysis to count objects over 0.1µm.

Immunofluorescence staining

Fixation and staining proceeded as in Lui-Roberts et al.[32]. Fixed cell images were taken on a Leica SPE scanning confocal microscope system with a 63x objective (NA 1.3) as confocal z-stacks with 0.5µm step size. Acquisition was performed using LAS-AF software with a 1024x1024 pixel resolution. 3-4 frame average and 1x zoom. To image clathrin recruitment, confluent HUVEC were stimulated +/- 100ng/ml PMA for 5 minutes then fixed in 4% PFA and stained for external VWF prior to permeabilising cells and staining for total VWF and clathrin. Cells were imaged as cross-sectional confocal y-stacks with a 0.5µm step size on a Leica SPE scanning confocal microscope system as above. For fixation following changes in pH, cells were cultured as before but stimulated in serum free media buffered with either 0.1M HEPES or 0.1M MES. Cells were fixed at 37°C in 4% methanol-free formaldehyde (TAAB Laboratories Equipment, Ltd.) in cytoskeleton buffer (10 mM MES, pH 6.1, 3 mM MgCl2, 138 mM KCl, and 2 mM EGTA) with 0.32M sucrose and then permeabilized in 0.5% Triton X-100 (Sigma) and incubated with Alexa Fluor 488–conjugated phalloidin (Life Technologies, Paisley, UK) and a relevant primary antibody.

Western blotting

Proteins were separated by SDS-PAGE, transferred to Whatman nitrocellulose membranes (PerkinElmer), and then probed with primary antibody followed by the appropriate HRP-conjugated secondary antibody (1:5000) purchased from Jackson ImmunoResearch Laboratories, Inc. (West Grove, PA, USA).

Imaging live dextran uptake

Transfected cells were seeded onto 8-well LabTek sterile borosilicate coverglass chamber slides (Life Technologies). After 24h chambers were rinsed with Ringer's solution (140mM NaCl, 5mM KCl, 1.8mM CaCl$_2$, 2mM MgCl$_2$, 10mM glucose, 20mM HEPES-NaOH pH 7.4) then mounted on a Leica TCS SP5 inverted microscope on a heated stage set at 37°C. Cells were stimulated with 100ng/ml PMA in the presence of 1mg/ml dextran-tetramethylrhodamine (Life Technologies,) and immediately imaged through a 63x oil immersion lens (NA 1.4) using an 8000hz high resonance scanner. Single confocal plane images (1024x1024 pixels) were taken every 5-10 seconds for 3-5 minutes using a single line and frame average.

Live cell imaging

For live cell imaging cells kd and untreated cells were transfected with GFP-VWF and mCherry-PselectinLum onto a glass bottom dish or for live cell CLEM a gridded coverslip bottom dish (in situations where exocytosis from kd cells was being monitored 300pmol AP-2 alpha siRNA was also included during the transfection). Imaging proceeded using a 100x oil immersion lens (NA 1.4) on a spinning-disk system (UltraVIEW VoX; Perkin-Elmer) mounted on an inverted microscope (TiE; Nikon, Kingston Upon Thames, UK) with an EM charge-couple device camera (512x512 pixels; C9100-13; Hamamatsu Photonics, Welwyn Garden City, UK) and 488 and 568 solid-state lasers. Z-stacks were acquired every 5s using a piezo (NanoSanZ; Prior Scientific, Cambridge, UK) with a step size of 0.4-0.5μm, comprising 9-14 images with an exposure of 30ms at either pH 7.4, pH 5.5 and in the presence or absence of 25μM dynasore (Sigma).

Correlative EM

Exocytic site labelling assays were carried out using a modified method described by Knop and Gerke, 2002[39]. Cells were cultured on gridded coverslip bottomed dishes (MatTek, Bratislava, Slovak Republic) and 24h later incubated for 10 minutes in the presence of rabbit anti-VWF +/- PMA (100ng/ml) either in the presence or absence of cytochalasin E (CCE) 1 μM or in the presence or absence of dynasore (25 μM) at pH 7.4 or at pH 5.5 (see IF protocol above, all from Sigma). In

experiments in which CCE was used the cells were pretreated for 15 minutes prior to stimulation. CLEM was carried out as in Nightingale *et al.*[24] For live cell imaging CLEM cells were transfected and imaged as above but beforehand the cell to be imaged was localised and DIC images acquired at 10x air (NA 0.3), 20x air (NA 0.7) and 40x (NA 0.75-1.25). At arbitrary time points 4X fix was added to the cells and images were acquired post fixation to confirm efficacy. The remainder of the TEM preparation was carried out as conventional CLEM.

Quantification of compensatory endocytic profiles by electron microscopy

Serial sections were arranged in order. Fused WPB were denoted by demonstrable loss of the mCherry-PselectinLum (in the case of correlative movie to electron microscopy) or the presence of gold labelled anti-VWF antibody at the cell surface and the presence of a collapsed structure (in non-correlative and correlative microscopy). Any ambiguous structures were excluded from the analysis. To be denoted as bona fide compensatory endocytic structures the budding vesicles had to have a demonstrable connection to the fused structure in at least one section. Tubular membrane structures such as endoplasmic reticulum (which are also often found near fusing WPB) were excluded as they occur in more than 1 or 2 sections and lack a clathrin coat.

String Analysis

HUVECs were seeded onto µ-slides (Ibidi, Munich, Germany) with a 5mm-wide channel 24 hours before experiments. HUVECs were pre-treated with 25µM dynasore for 15 minutes or left untreated and slides subsequently attached to a syringe pump (Harvard Apparatus, Holliston, MA, USA) to draw fluid over the cells at a constant wall shear stress of 0.25MPa (2.5 dynes/cm^2). Cells were maintained at 37°C and were perfused with buffer (Hanks balanced salt solution (HBSS, Life Technologies) containing Ca^{2+}, Mg^{2+} and 0.2% BSA) for two minutes to remove debris before being stimulated with PMA (100ng/ml) in the presence or absence of dynasore for five minutes in HBSS buffer (as above). Cells were fixed with 4% PFA under decreasing rates of flow for 10 minutes until static and left in PFA for a further 10 minutes. Samples were prepared for immunofluorescence without permeabilisation, and stained for surface-bound VWF via incubation with rabbit anti-VWF (DAKO) followed by Alexa 488-conjugated anti-rabbit secondary antibody and stained for the nucleus with Hoechst 33342 (Life Technologies). VWF strings were imaged by confocal microscopy (Leica TCS SPE) using a 40x (NA 1.15) oil objective. Maximum intensity projections were generated of confocal stacks in Fiji that were used to manually count VWF strings.

Competing interests

No authors have any competing interests.

Author contributions

Contribution: T.D.N., N.L.S., J.J.M., C.R. and I.J.W. designed research, performed research, analysed research and wrote paper. D.F.C. Designed research analysed research and wrote paper.

References

1.   Burgoyne RD, Morgan A. Secretory granule exocytosis. *Physiol Rev*. 2003;83(2):581-632.
2.   Nightingale TD, Cutler DF, Cramer LP. Actin coats and rings promote regulated exocytosis. *Trends Cell Biol*. 2012;22(6):329-337.
3.   Thorn P, Zorec R, Rettig J, Keating DJ. Exocytosis in non-neuronal cells. *J Neurochem*. 2016;137(6):849-859.
4.   Barg S, Machado JD. Compensatory endocytosis in chromaffin cells. *Acta Physiol (Oxf)*. 2008;192(2):195-201.
5.   Soykan T, Maritzen T, Haucke V. Modes and mechanisms of synaptic vesicle recycling. *Curr Opin Neurobiol*. 2016;39:17-23.
6.   Gordon SL, Cousin MA. The iTRAPs: Guardians of Synaptic Vesicle Cargo Retrieval During Endocytosis. *Front Synaptic Neurosci*. 2016;8:1.
7.   Reider A, Wendland B. Endocytic adaptors--social networking at the plasma membrane. *J Cell Sci*. 2011;124(Pt 10):1613-1622.
8.   Okamoto Y, Lipstein N, Hua Y, et al. Distinct modes of endocytotic presynaptic membrane and protein uptake at the calyx of Held terminal of rats and mice. *Elife*. 2016;5.
9.   Watanabe S, Rost BR, Camacho-Perez M, et al. Ultrafast endocytosis at mouse hippocampal synapses. *Nature*. 2013;504(7479):242-247.
10.   Watanabe S, Trimbuch T, Camacho-Perez M, et al. Clathrin regenerates synaptic vesicles from endosomes. *Nature*. 2014;515(7526):228-233.
11.   Willox AK, Royle SJ. Stonin 2 is a major adaptor protein for clathrin-mediated synaptic vesicle retrieval. *Curr Biol*. 2012;22(15):1435-1439.
12.   Henkel AW, Almers W. Fast steps in exocytosis and endocytosis studied by capacitance measurements in endocrine cells. *Curr Opin Neurobiol*. 1996;6(3):350-357.
13.   Ryan TA. Kiss-and-run, fuse-pinch-and-linger, fuse-and-collapse: the life and times of a neurosecretory granule. *Proc Natl Acad Sci U S A*. 2003;100(5):2171-2173.
14.   Artalejo CR, Henley JR, McNiven MA, Palfrey HC. Rapid endocytosis coupled to exocytosis in adrenal chromaffin cells involves Ca2+, GTP, and dynamin but not clathrin. *Proc Natl Acad Sci U S A*. 1995;92(18):8328-8332.
15.   Holroyd P, Lang T, Wenzel D, De Camilli P, Jahn R. Imaging direct, dynamin-dependent recapture of fusing secretory granules on plasma membrane lawns from PC12 cells. *Proc Natl Acad Sci U S A*. 2002;99(26):16806-16811.
16.   Lenting PJ, Christophe OD, Denis CV. von Willebrand factor biosynthesis, secretion, and clearance: connecting the far ends. *Blood*. 2015;125(13):2019-2028.
17.   Nightingale T, Cutler D. The secretion of von Willebrand factor from endothelial cells; an increasingly complicated story. *J Thromb Haemost*. 2013;11 Suppl 1:192-201.
18.   Valentijn KM, Eikenboom J. Weibel-Palade bodies: a window to von Willebrand disease. *J Thromb Haemost*. 2013;11(4):581-592.
19.   Ferraro F, Mafalda Lopes da S, Grimes W, et al. Weibel-Palade body size modulates the adhesive activity of its von Willebrand Factor cargo in cultured endothelial cells. *Sci Rep*. 2016;6:32473.
20.   Springer TA. von Willebrand factor, Jedi knight of the bloodstream. *Blood*. 2014;124(9):1412-1425.
21.   Dong JF, Moake JL, Nolasco L, et al. ADAMTS-13 rapidly cleaves newly secreted ultralarge von Willebrand factor multimers on the endothelial surface under flowing conditions. *Blood*. 2002;100(12):4033-4039.
22.   Erent M, Meli A, Moisoi N, et al. Rate, extent and concentration dependence of histamine-evoked Weibel-Palade body exocytosis determined from individual fusion events in human endothelial cells. *J Physiol*. 2007;583(Pt 1):195-212.
23.   Han X, Li P, Yang Z, et al. Zyxin regulates endothelial von Willebrand factor secretion by reorganizing actin filaments around exocytic granules. *Nat Commun*. 2017;8:14639.

24.   Nightingale TD, White IJ, Doyle EL, et al. Actomyosin II contractility expels von Willebrand factor from Weibel-Palade bodies during exocytosis. *J Cell Biol*. 2011;194(4):613-629.

25.   James PD, Lillicrap D. The molecular characterization of von Willebrand disease: good in parts. *Br J Haematol*. 2013;161(2):166-176.

26.   Bonfanti R, Furie BC, Furie B, Wagner DD. PADGEM (GMP140) is a component of Weibel-Palade bodies of human endothelial cells. *Blood*. 1989;73(5):1109-1112.

27.   McEver RP, Beckstead JH, Moore KL, Marshall-Carlson L, Bainton DF. GMP-140, a platelet alpha-granule membrane protein, is also synthesized by vascular endothelial cells and is localized in Weibel-Palade bodies. *J Clin Invest*. 1989;84(1):92-99.

28.   Valentijn KM, van Driel LF, Mourik MJ, et al. Multigranular exocytosis of Weibel-Palade bodies in vascular endothelial cells. *Blood*. 2010;116(10):1807-1816.

29.   Zupancic G, Ogden D, Magnus CJ, Wheeler-Jones C, Carter TD. Differential exocytosis from human endothelial cells evoked by high intracellular Ca(2+) concentration. *J Physiol*. 2002;544(Pt 3):741-755.

30.   Babich V, Meli A, Knipe L, et al. Selective release of molecules from Weibel-Palade bodies during a lingering kiss. *Blood*. 2008;111(11):5282-5290.

31.   Mourik MJ, Valentijn JA, Voorberg J, Koster AJ, Valentijn KM, Eikenboom J. von Willebrand factor remodeling during exocytosis from vascular endothelial cells. *J Thromb Haemost*. 2013;11(11):2009-2019.

32.   Lui-Roberts WW, Collinson LM, Hewlett LJ, Michaux G, Cutler DF. An AP-1/clathrin coat plays a novel and essential role in forming the Weibel-Palade bodies of endothelial cells. *J Cell Biol*. 2005;170(4):627-636.

33.   Michaux G, Abbitt KB, Collinson LM, Haberichter SL, Norman KE, Cutler DF. The physiological function of von Willebrand's factor depends on its tubular storage in endothelial Weibel-Palade bodies. *Dev Cell*. 2006;10(2):223-232.

34.   Arribas M, Cutler DF. Weibel-Palade body membrane proteins exhibit differential trafficking after exocytosis in endothelial cells. *Traffic*. 2000;1(10):783-793.

35.   Babich V, Knipe L, Hewlett L, et al. Differential effect of extracellular acidosis on the release and dispersal of soluble and membrane proteins secreted from the Weibel-Palade body. *J Biol Chem*. 2009;284(18):12459-12468.

36.   Rondaij MG, Bierings R, Kragt A, van Mourik JA, Voorberg J. Dynamics and plasticity of Weibel-Palade bodies in endothelial cells. *Arterioscler Thromb Vasc Biol*. 2006;26(5):1002-1007.

37.   Zografou S, Basagiannis D, Papafotika A, et al. A complete Rab screening reveals novel insights in Weibel-Palade body exocytosis. *J Cell Sci*. 2012;125(Pt 20):4780-4790.

38.   Hannah MJ, Skehel P, Erent M, Knipe L, Ogden D, Carter T. Differential kinetics of cell surface loss of von Willebrand factor and its propolypeptide after secretion from Weibel-Palade bodies in living human endothelial cells. *J Biol Chem*. 2005;280(24):22827-22830.

39.   Knop M, Aareskjold E, Bode G, Gerke V. Rab3D and annexin A2 play a role in regulated secretion of vWF, but not tPA, from endothelial cells. *EMBO J*. 2004;23(15):2982-2992.

40.   Macia E, Ehrlich M, Massol R, Boucrot E, Brunner C, Kirchhausen T. Dynasore, a cell-permeable inhibitor of dynamin. *Dev Cell*. 2006;10(6):839-850.

41.   Motley A, Bright NA, Seaman MN, Robinson MS. Clathrin-mediated endocytosis in AP-2-depleted cells. *J Cell Biol*. 2003;162(5):909-918.

42.   Motley AM, Berg N, Taylor MJ, et al. Functional analysis of AP-2 alpha and mu2 subunits. *Mol Biol Cell*. 2006;17(12):5298-5308.

43.   Houy S, Croise P, Gubar O, et al. Exocytosis and endocytosis in neuroendocrine cells: inseparable membranes! *Front Endocrinol (Lausanne)*. 2013;4:135.

44.   Zenner HL, Collinson LM, Michaux G, Cutler DF. High-pressure freezing provides insights into Weibel-Palade body biogenesis. *J Cell Sci*. 2007;120(Pt 12):2117-2125.

45. Lui-Roberts WW, Ferraro F, Nightingale TD, Cutler DF. Aftiphilin and gamma-synergin are required for secretagogue sensitivity of Weibel-Palade bodies in endothelial cells. *Mol Biol Cell*. 2008;19(12):5072-5081.

46. Hua Y, Woehler A, Kahms M, Haucke V, Neher E, Klingauf J. Blocking endocytosis enhances short-term synaptic depression under conditions of normal availability of vesicles. *Neuron*. 2013;80(2):343-349.

47. Jung S, Maritzen T, Wichmann C, et al. Disruption of adaptor protein 2mu (AP-2mu) in cochlear hair cells impairs vesicle reloading of synaptic release sites and hearing. *EMBO J*. 2015;34(21):2686-2702.

48. Pulido IR, Jahn R, Gerke V. VAMP3 is associated with endothelial weibel-palade bodies and participates in their Ca(2+)-dependent exocytosis. *Biochim Biophys Acta*. 2011;1813(5):1038-1044.

49. Behrendorff N, Dolai S, Hong W, Gaisano HY, Thorn P. Vesicle-associated membrane protein 8 (VAMP8) is a SNARE (soluble N-ethylmaleimide-sensitive factor attachment protein receptor) selectively required for sequential granule-to-granule fusion. *J Biol Chem*. 2011;286(34):29627-29634.

50. Pickett JA, Edwardson JM. Compound exocytosis: mechanisms and functional significance. *Traffic*. 2006;7(2):109-116.

51. Alvarez de Toledo G, Fernandez JM. Compound versus multigranular exocytosis in peritoneal mast cells. *J Gen Physiol*. 1990;95(3):397-409.

52. Nemoto T, Kimura R, Ito K, et al. Sequential-replenishment mechanism of exocytosis in pancreatic acini. *Nat Cell Biol*. 2001;3(3):253-258.

53. Thorn P, Parker I. Two phases of zymogen granule lifetime in mouse pancreas: ghost granules linger after exocytosis of contents. *J Physiol*. 2005;563(Pt 2):433-442.

54. Kiskin NI, Babich V, Knipe L, Hannah MJ, Carter T. Differential cargo mobilisation within Weibel-Palade bodies after transient fusion with the plasma membrane. *PLoS One*. 2014;9(9):e108093.

55. Romani de Wit T, Rondaij MG, Hordijk PL, Voorberg J, van Mourik JA. Real-time imaging of the dynamics and secretory behavior of Weibel-Palade bodies. *Arterioscler Thromb Vasc Biol*. 2003;23(5):755-761.
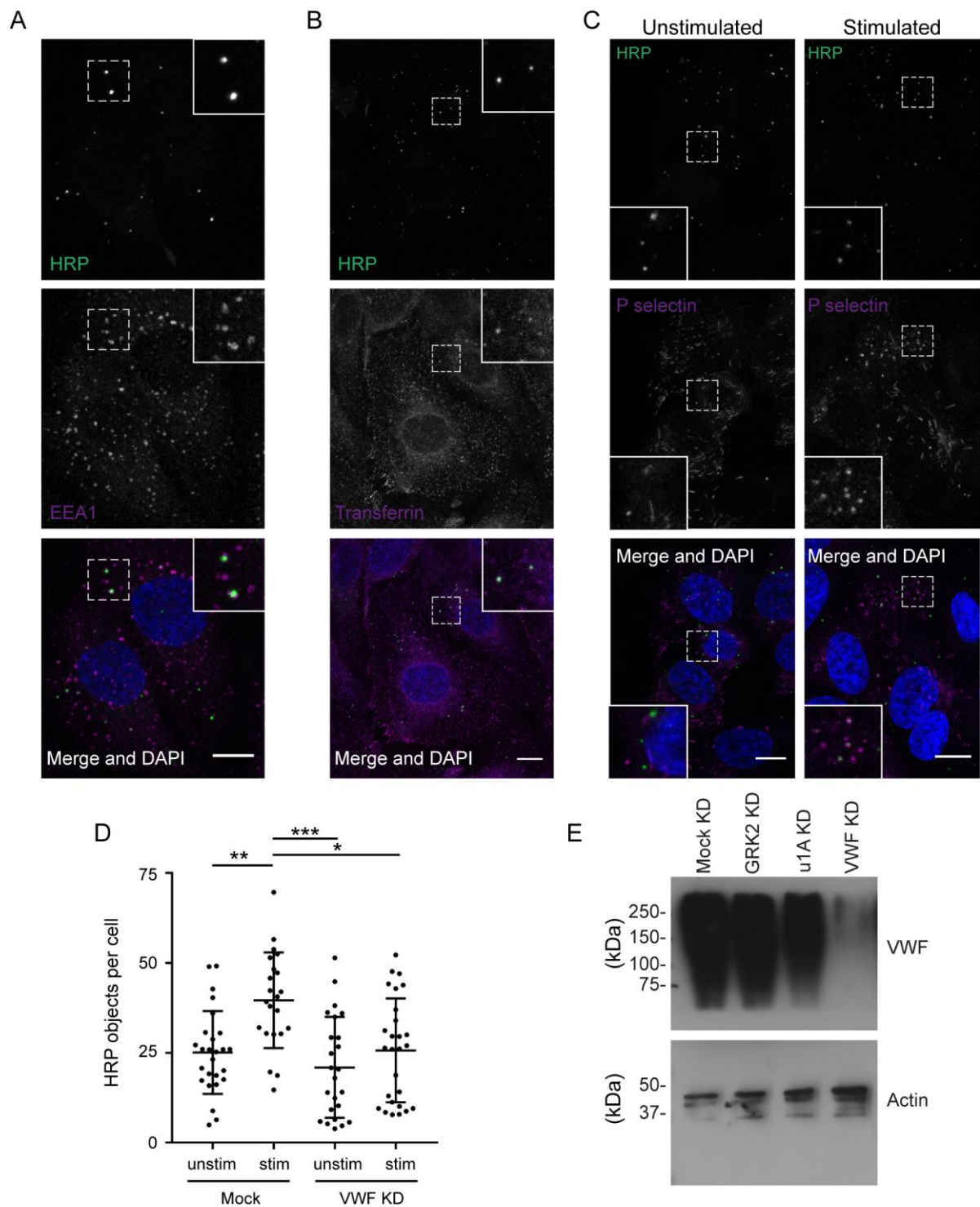
Figure 1. **Analysis of the extent of WPB specific compensatory endocytosis**

(A) HUVEC were fed for 15 minutes with soluble HRP then fixed and stained for HRP (green) and EEA-1 (magenta). The nucleus is labelled with DAPI (Blue). HRP and EEA1 co-localise, as indicated by

white pixels, demonstrating HRP is within endosomes. (B) HUVEC were incubated with Alexa 568nm fluorescently tagged transferrin (magenta) for two minutes, washed and then uptake chased for 15 minutes in the presence of HRP (green). HRP and transferrin co-localise. (C) HUVEC fed with HRP (green) in the absence (left) or presence (right) of 100ng/ml PMA for 10 minutes were fixed and stained for P-selectin. In unstimulated cells, P-selectin is stored within rod-shaped WPBs and does not localize with HRP. Following stimulation, P-selectin is present on round endocytic vesicles positive for HRP demonstrating it has been retrieved from the cell surface. (A-C) Images shown are maximum intensity projections and boxed areas contain zooms of the regions of interest denoted by dashed outline. Scale bars are 20 μm. (D) Cells transfected with control or VWF siRNA were incubated with HRP +/- 100ng/ml PMA for 15 minutes and then treated as above. A 70% increase in HRP positive objects is seen upon stimulation in control, but not VWF KD, cells (n=3). Error bars represent SEM. Stats shown derived from student's T test (P=<0.05) (E) Mock treated and cells depleted for GRK2, the AP-1 subunit μ1A or VWF were lysed and the levels of VWF and actin determined by SDS PAGE and western blot. GRK-2 is required for controlling regulation of GPCR signaling whilst the AP-1 subunit μ1A is required for normal WPB formation. Only depletion of VWF itself effects total VWF levels.
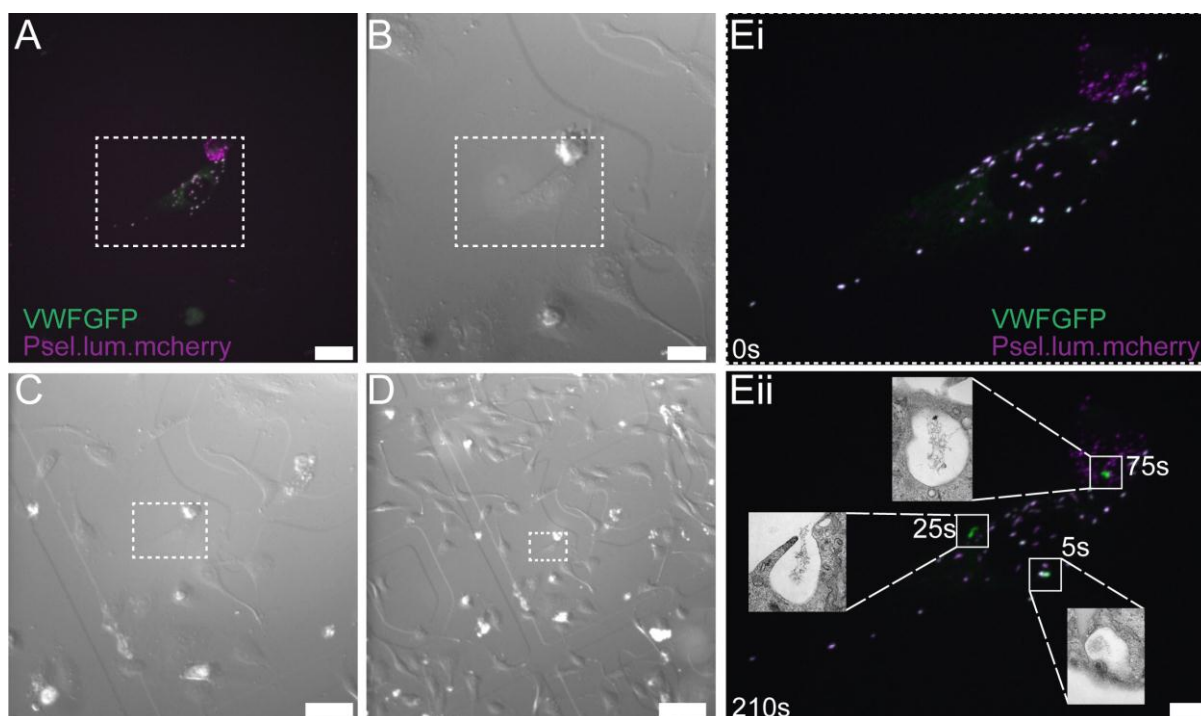
Figure 2. **Correlative live cell imaging and electron microscopy to monitor kinetics and ultrastructure of compensatory endocytosis**

HUVEC were transfected with mCherry-PselectinLum (magenta) and GFP-VWF and plated on gridded coverslip bottomed dishes. (A) Fluorescent cells were identified (maximum intensity projection is shown) and DIC images acquired at (B) 40x (C) 20X and (D) 10X magnifications to define localisation in x and y as denoted by the boxed region. Scale bar (A & B) 20 (C) 50 (D) 100 µm. Transfected cells were then stimulated with 100ng/ml PMA and the same cell imaged by spinning disc microscopy before fixation at arbitrary time points. (E) Images show the cell at (i) 0s and (ii) 210s. Fused WPB release the mCherry (magenta) marker at the point of fusion and then more gradually release GFP-VWF during content release. (Eii) Inserts show TEM images of the specific exit sites indicated. Time points shown represent time between loss of fusion marker and point of fixation. Scale bar 10 µm.
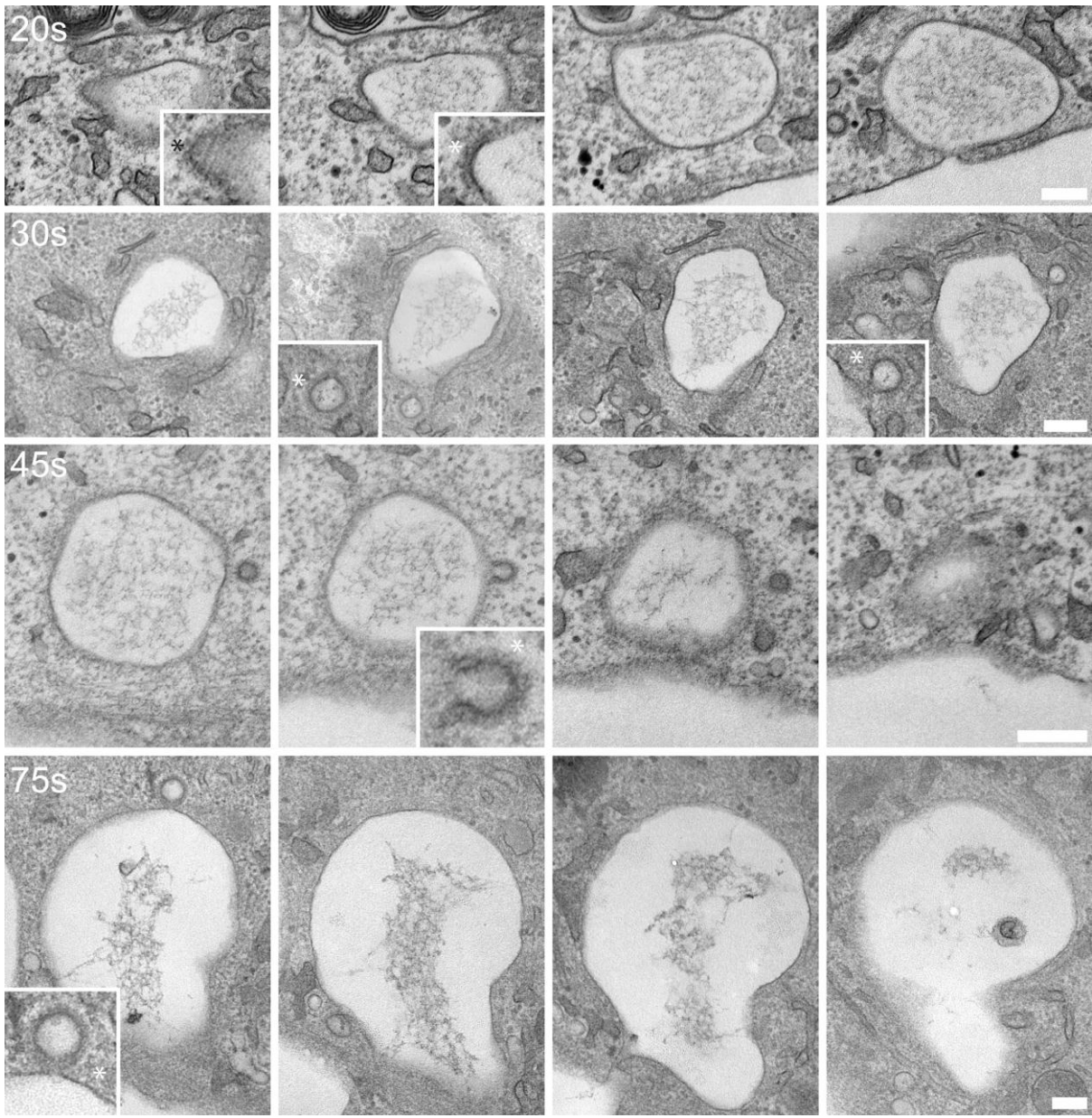
Figure 3. Ultrastructure of compensatory endocytic events following WPB fusion

HUVEC were co-transfected with mCherry-PselectinLum and GFP-VWF before performing live cell imaging and CLEM. All images shown are 70nm thick serial sections through individual fused WPB fixed at different timepoints post-fusion as shown at the top left of each image series. Asterisks indicate examples of compensatory structures. Inserts show zoom of compensatory structures. The earliest time that compensatory structures are noted is 20s post fusion and all such structures are clathrin coated. Representative images are taken from n=6 experiments, scale bar 200nm.
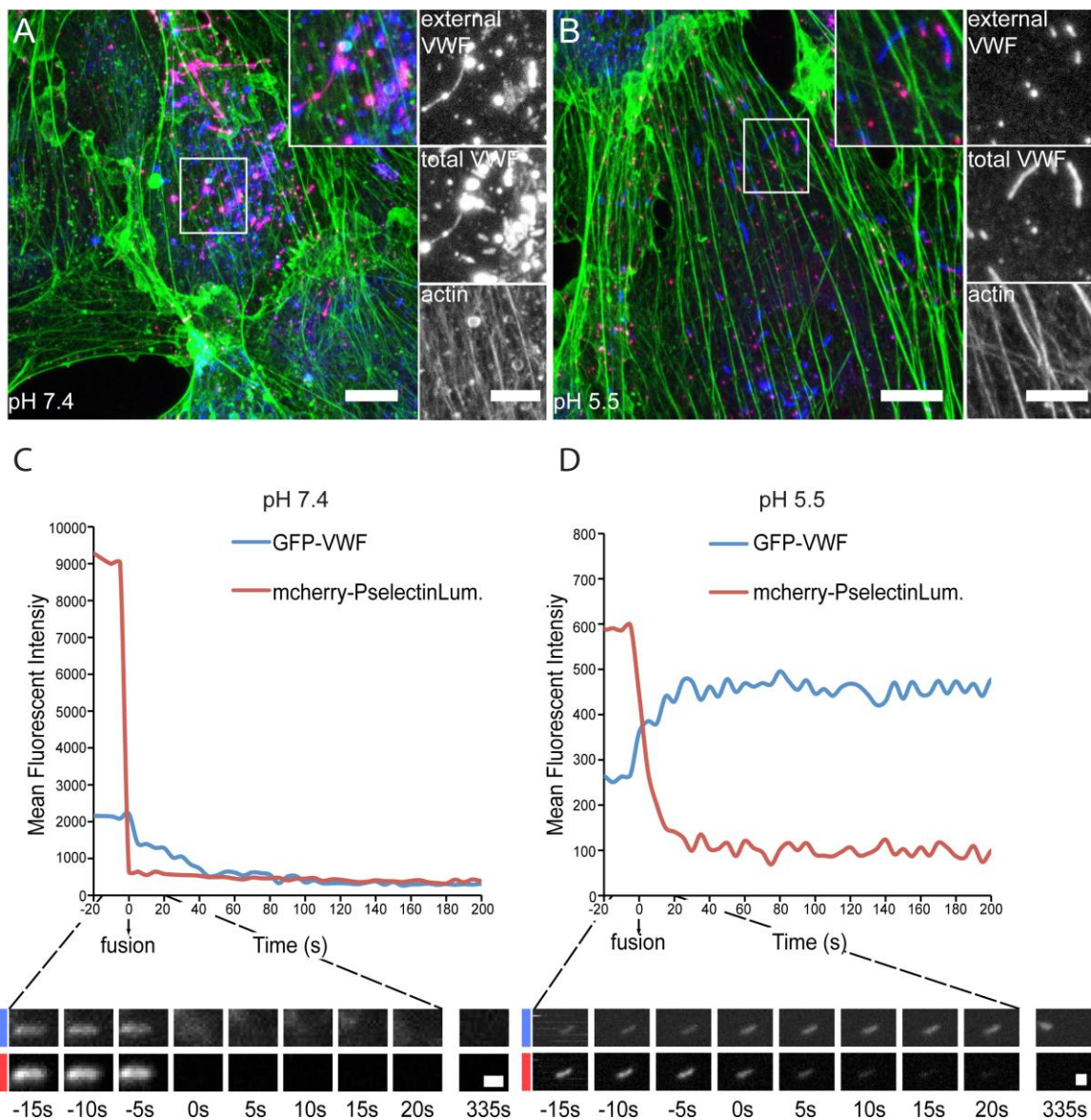
Figure 4. **Effect of low pH on WPB fusion**

(A & B) HUVEC were stimulated with PMA (100ng/ml) for 10 minutes in (A) pH 7.4 or (B) pH 5.5 medium. Cells were labelled for external VWF (magenta) total VWF (blue) and for the actin cytoskeleton (green). Images shown are maximum intensity projections. Scale bar 10 μm. The boxed area is shown magnified in the inserts. Scale bar 5 μm. (C & D) HUVEC were co-transfected with mCherry-PselectinLum and GFP-VWF before PMA stimulation (100ng/ml) at (C) pH 7.4 or (D) pH 5.5. Graphs indicate changes in mean fluorescent intensity 20 seconds before fusion and 200 seconds post fusion for the representative individual WPB shown below at each time point. At pH 7.4 WPB collapse and lose content. At pH 5.5 fused WPB lose the marker for fusion but retain VWF and stay rod shaped. Images show individual slices and scale bar is 1 μm.
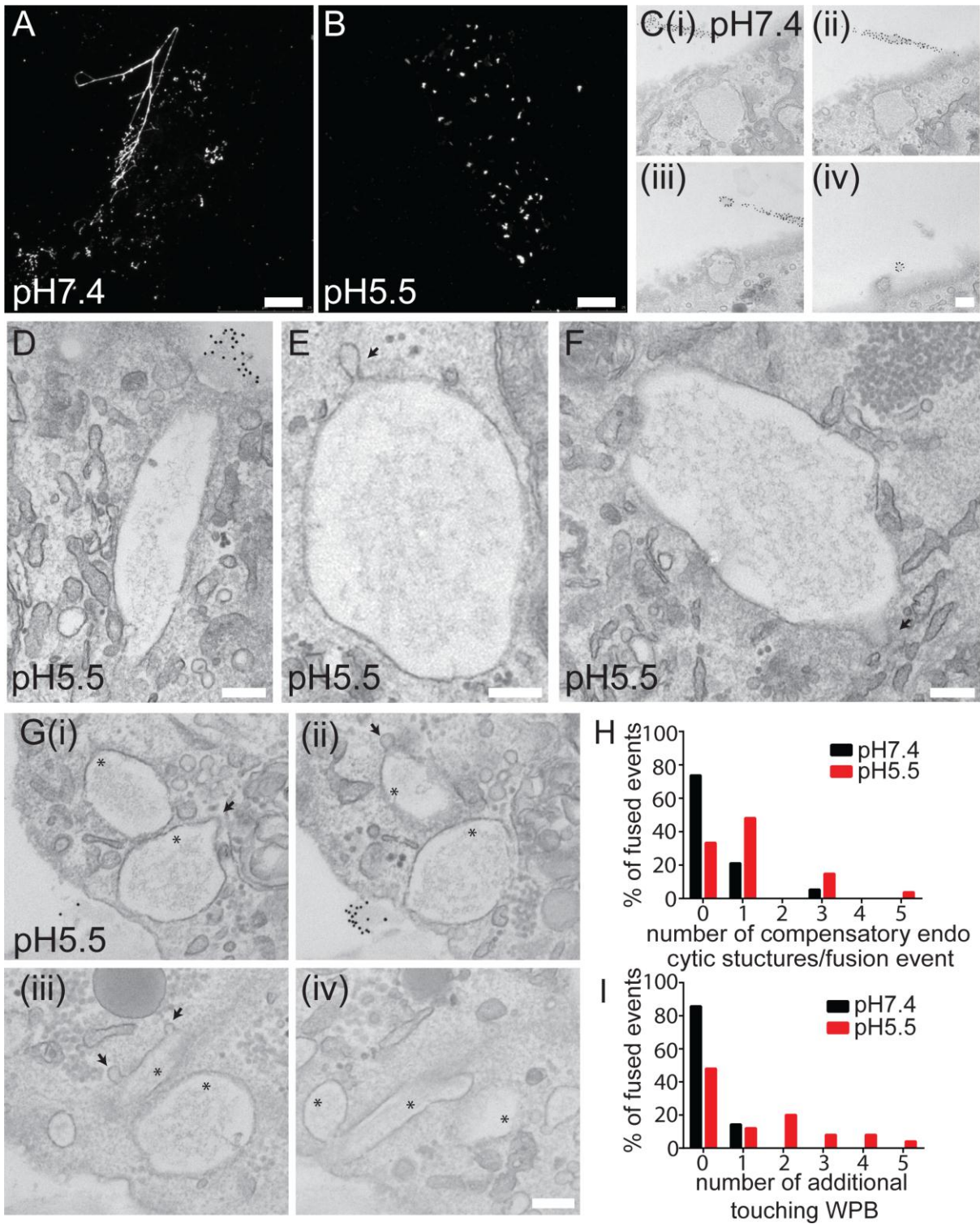
Figure 5. **Correlative electron microscopy of WPB fusion at low pH**

HUVEC were stimulated with PMA (100ng/ml) for 10 minutes in pH 7.4 (A & C) or pH 5.5 (B & D-G) medium. Cells were then fixed and external VWF labelled with anti-VWF antibodies and a

combination of Alexa 488nm and 10nm protein A gold before imaging by confocal microscopy (A & B, maximum intensity projections, scale bar 10 μm), and preparation for CLEM (C-G, 70 nm serial sections, scale bar 200nm). (A & C) At neutral pH WPB collapse and strings of VWF are clearly visible. (B & D-F) At pH 5.5 WPB retain tubulated VWF and WPB vary from completely collapsed to entirely rod shaped (all WPB shown were fused as indicated by the presence of external gold labelling-not shown, arrows show compensatory encocytic structures). (G) Cumulative fusion events are apparent at pH5.5. Arrows show compensatory endocytic structures, asterisks indicate fused collapsed WPB. (H) Quantification of the distribution of compensatory endocytic profiles at pH 7.4 and pH 5.5. At pH 7.4 most profiles lack compensatory structures but at pH 5.5 nearly 70% still have compensatory endocytic structures present. Data is pooled from n=4 experiments. (I) EM quantification of the prevalence of cumulative exocytosis at pH 5.5 and pH 7.4. TEM images in which fused (as evidenced by gold labelling) WPB membranes were clearly touching other collapsed or unfused WPB were classed as cumulative. Data is pooled from n=4 experiments.
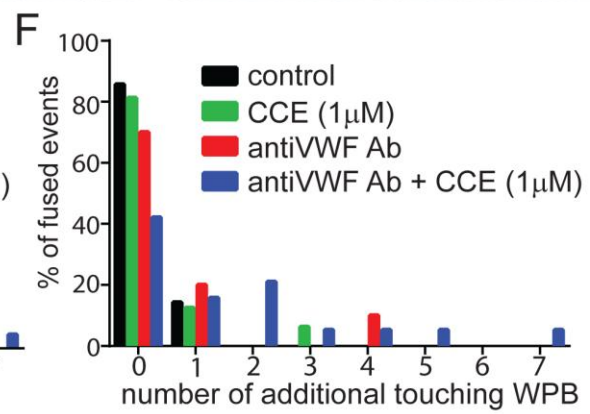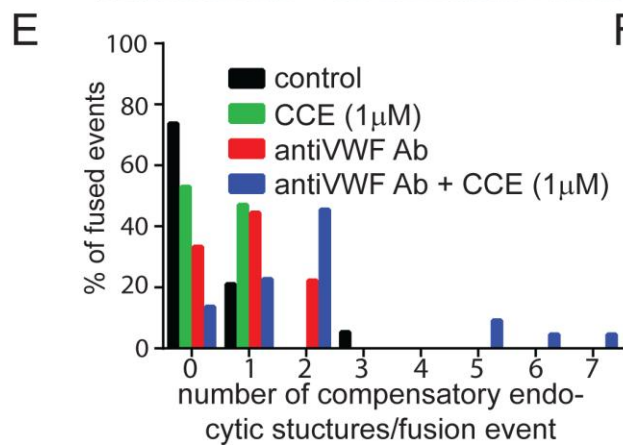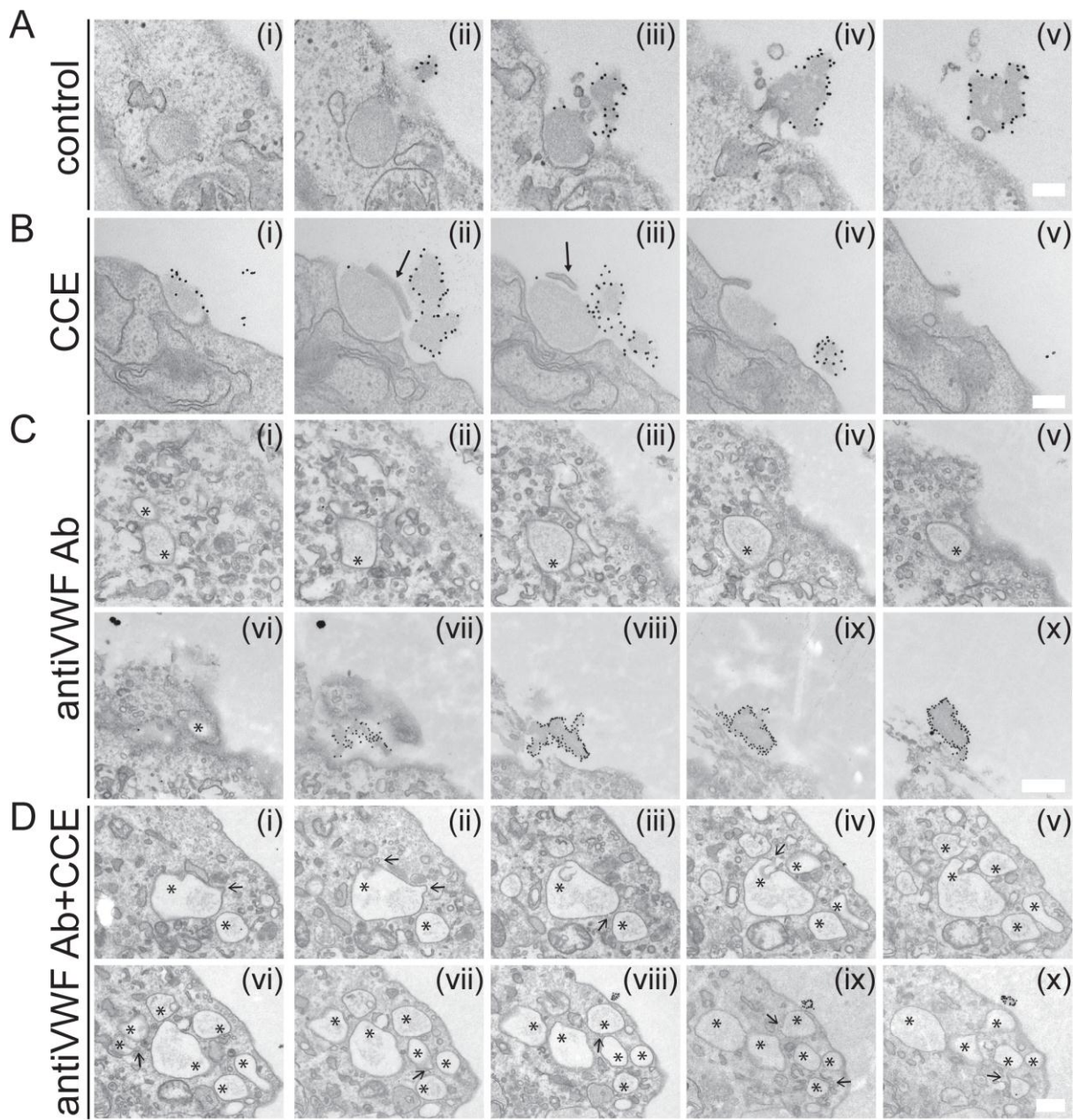
Figure 6. **Reduction in the rate of content release is correlated with increased compensatory endocytosis and cumulative exocytosis**

HUVEC were stimulated with PMA (100ng/ml) for 10 minutes (A) in media, or media supplemented with (B) 1µM cytochalasin E (CCE), (C) anti-VWF antibody (1 in 500) or (D) both agents together. Cells were then fixed and external VWF labelled with anti-VWF antibodies before preparation for TEM. Image series are from serial sectioning, scale bar A & B-200nm, C & D-500nm. Arrows with solid heads show pieces of membrane still covering the pore, open arrows show compensatory endocytic structures, asterisks indicate fused collapsed WPB. (E) Quantification of the distribution of compensatory endocytic profiles following stimulation in control conditions and in the presence of CCE, antibody (Ab) or Ab + CCE. (F) EM quantification of the prevalence of cumulative exocytosis in the presence of CCE, Ab or Ab + CCE. TEM images in which fused (as evidenced by gold labelling) WPB membranes were clearly touching other collapsed or unfused WPB were classed as in the process of cumulative fusion. Data is pooled from n=10 control, n=6 CCE and n=3 Ab + CCE experiments. Cumulative exocytosis is associated with an increase in compensatory exocytosis and is most prevalent when antibody is present in the medium and the actin ring is depolymerised.
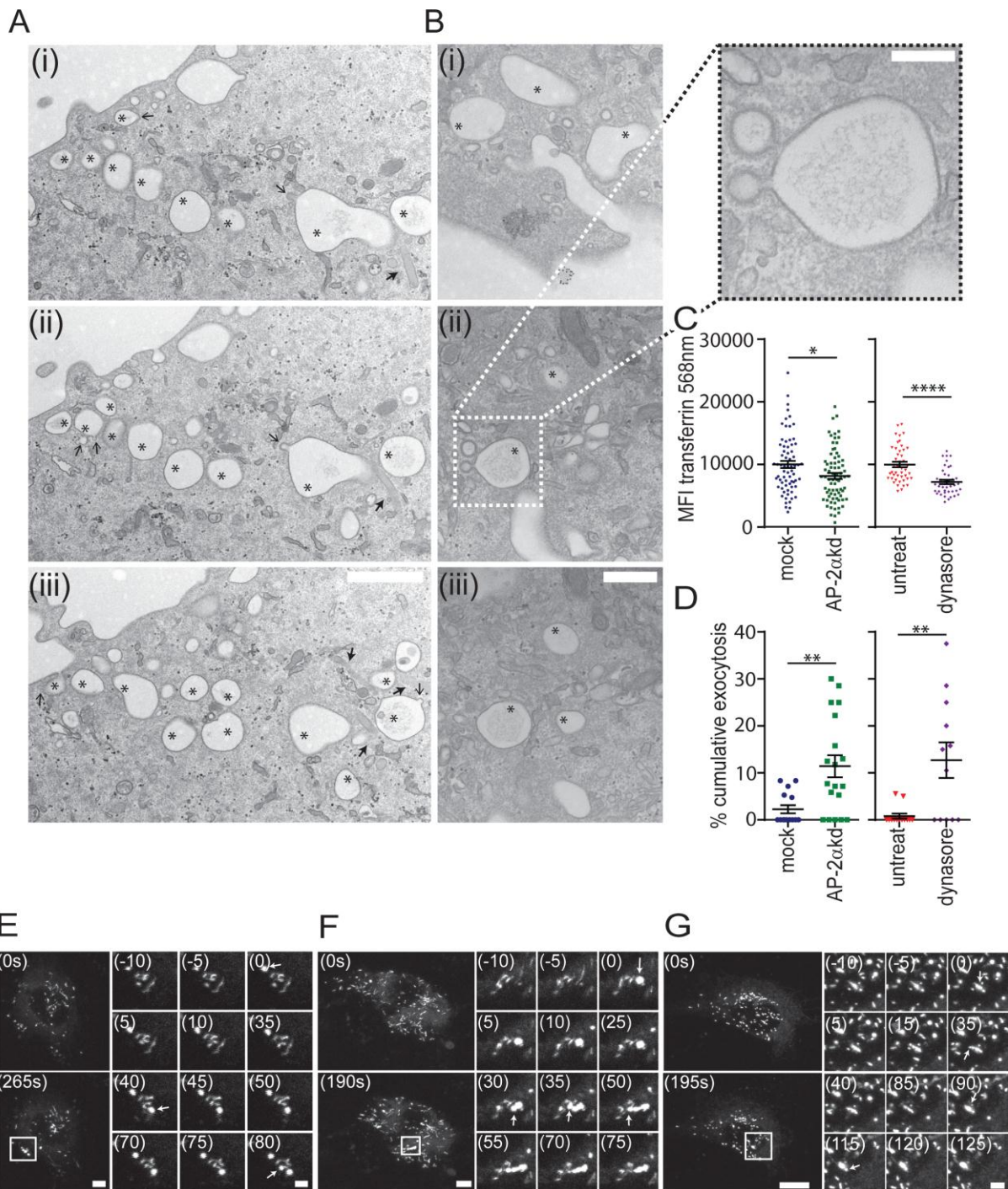
Figure 7. **Inhibition of compensatory endocytosis increases the likelihood of cumulative exocytosis**

(A-F) HUVEC were pre-incubated with control media or 25µM dynasore supplemented media for 15 minutes before stimulation with 100ng/ml PMA. (A, B) Cells were fixed after 10 minutes and prepared for TEM. Representative serial sections show multiple collapsed WPB (denoted by asterisks) with membranes touching projecting from the cell surface into the cytoplasm. Unfused

WPB (denoted by solid arrow heads) are also seen touching these collapsed structures. Open arrows show compensatory endocytic structures (B) The boxed area is shown at a higher magnification showing two clathrin coated compensatory endocytic structures with wide necks. This likely reflects inhibited dynamin pinch-ase function. Scale bar A-1µm, B-500nm & B insert-200nm. (C) Untreated, dynasore or AP-2 alpha kd cells treated cells were fed with Alexa 568nm labelled transferrin for 15 minutes. The mean fluorescence intensity of each cell over background was determined using Image J software (control=45 cells, dynasore=40 cells, mock=69 cells, Ap-2= 75 cells pooled from 4 experiments, error bars represent SEM, t-test, *$P<0.05$, ****$P<0.0001$). (D-G) control (E, F) or AP-2 alpha kd (G) HUVEC were transfected with GFP-VWF and pre-incubated with (E & G) control media or (F) 25µM dynasore supplemented media for 15 minutes, before stimulation with 100ng/ml PMA and imaging for 10 minutes on a scanning confocal microscope. (D) Quantification of cumulative exocytosis in the presence and absence of 25µM dynasore (n=13 control n=13 dynasore treated cells, n=15 mock treated cells and n=19 AP-2 alpha kd cells from 4 experiments). Error bars represent SEM. Stats shown derived from student's T test ($P=<0.005$). Representative images of (E) untreated cells at 0 and 265s, (F) Dynasore treated cells at 0 and 190s post stimulation are shown (G) AP-2 alpha kd cells at 0 and 195s. Scale bar 10µm. Insets show the boxed region magnified (scale bar 2µm), with the time in the top left representing the time of the first fusion event. Arrows indicate point of WPB fusion. (E) In control cells, despite fusion events occurring in close proximity, and within 80s, the sites remain separate. (F) Fusion events occurring in close proximity and within 75s in dynasore treated or within 125s in AP-2kd cells merge in what appears to be cumulative exocytosis.
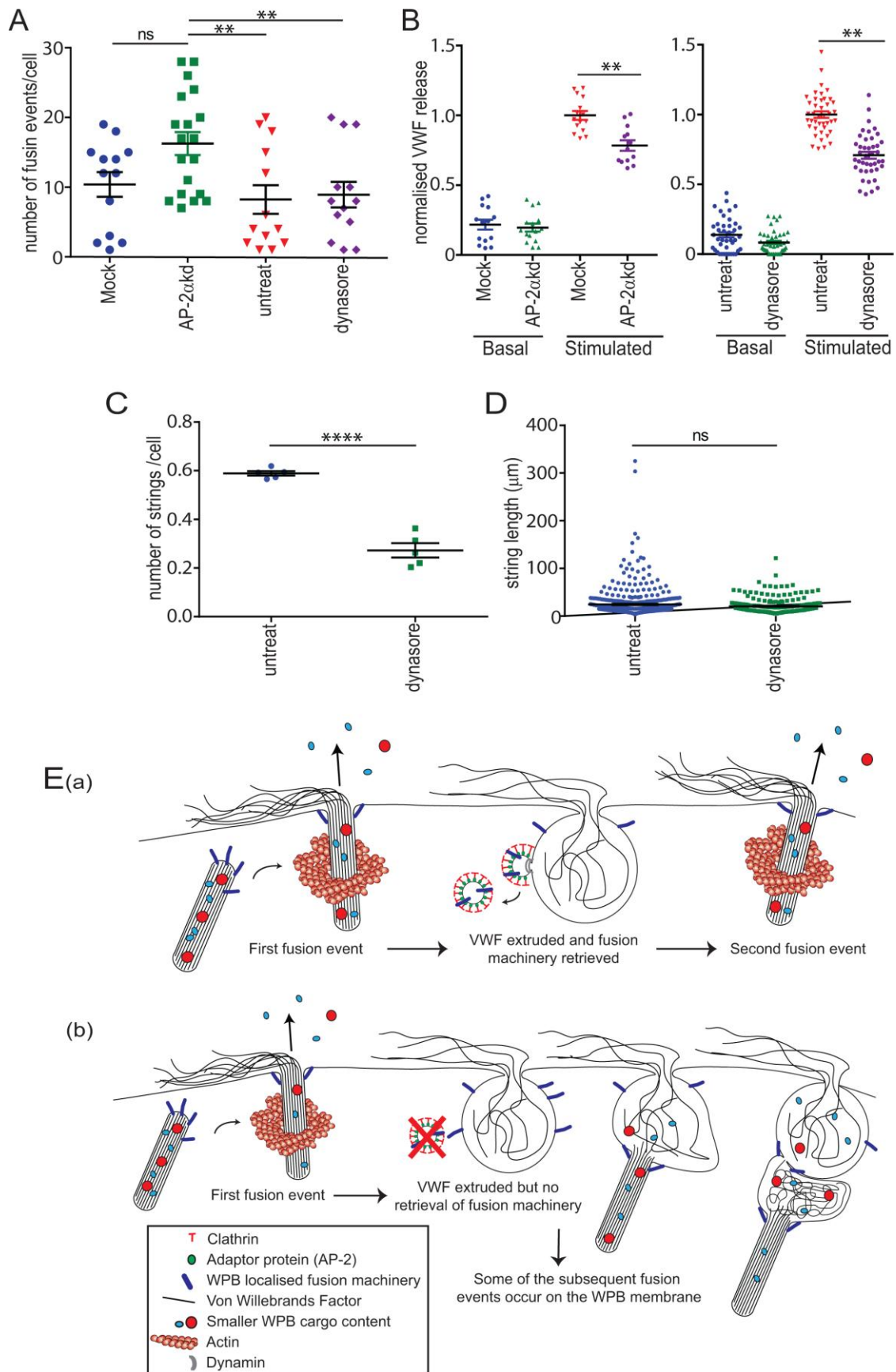
Figure 8. **Cumulative fusion of WPB results in improper release of VWF strings**

(A-B) Control, mock, 25µM dynasore treated or AP-2 alpha kd HUVEC were stimulated with 100ng/ml PMA. (A) The number of fusion events were monitored over a 10 minute period by scanning confocal microscopy. There was no significant difference in the extent of fusion between dynasore treated and untreated cells (n=13 control and drug treated cells from 4 experiments). A significant difference in the amount of fusion was noted in AP-2 kd compared to mock, control and dynasore treated cells. Error bars represent SEM. Stats shown derived from student's T test, P=<0.005. (B) Treated, dynasore treated mock and AP-2 alpha kd cells were incubated in the presence or absence of PMA (100ng/ml) and the amount of VWF release determined by ELISA as a fraction of total VWF. Data is normalised to control and there is a small but significant inhibition of VWF release noted. Error bars represent SEM, 1-way ANOVA with Kruskall-Wallis post-test, p<0.001, data shown represents 6 individual measurements from n=7 dynasore or n=5 AP-2 kd experiments. (C & D) Dynasore treated or untreated cells were stimulated under flow with 100ng/ml PMA and (C) the number and (D) length of VWF strings determined. Representative data shown from n=3 experiments error bars represent SEM. Stats shown derived from unpaired student's T test (P=<0.0001). (E) Model of the mechanism and function of compensatory endocytosis in endothelial cells: (a) WPB dock and fuse with the plasma membrane releasing VWF strings as well as smaller soluble and membrane bound cargo. The majority of WPB exocytic events do not result in full fusion i.e. total collapse of the organelle into the plasma membrane. Instead, fused empty WPB persist as distinct structures on which clathrin-coated budding vesicles assemble as early as 20 seconds post exocytosis. The formation of AP-2 mediated clathrin-coated vesicles occurs irrespective of whether the pore is open and such events serve to retrieve fusion machinery in a dynamin and AP-2 dependent manner. The fusion pores close after approximately 60-75s whilst clathrin-mediated budding continues; (b) When clathrin mediated endocytosis is inhibited either via inhibition of AP-2 or dynamin this causes WPB fusion machinery to build up on the post-fusion granule membrane. This makes such sites favourable for WPB fusion causing cumulative exocytosis. VWF released from such cumulative events cannot unfurl properly under flow and becomes tangled, resulting in shorter strings.
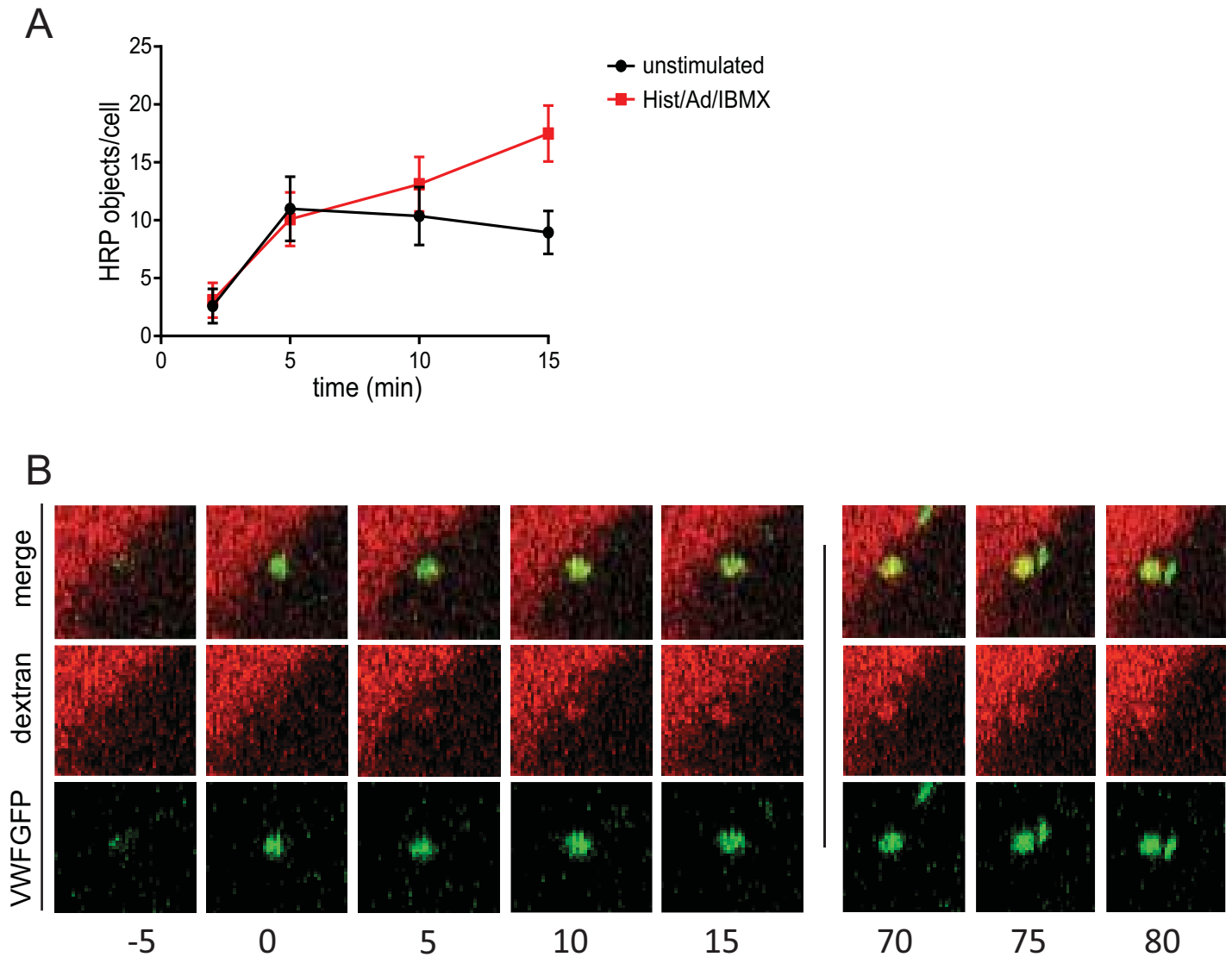
Supplementary Figures

A

B

Figure S1. Live cell imaging of dextran incorporation into fused WPB

(A) HUVEC were incubated with HRP +/- a cocktail of Histamine (100µM), Adrenaline (10µM) and IBMX (100 µM) for 15 minutes. The number of HRP positive objects/cell was determined and plotted relative to time. (B) HUVECs expressing VWF-GFP (green) were imaged live in the presence of PMA (100ng/ml) and dextran-tetramethylrhodamine (red). One representative exocytic event is presented, which occurs at relative time 0 (time indicated underneath pictures in seconds). Images are single confocal planes. The fusion pore can be seen to fill with dextran, whereas a second WPB, which comes into focus and does not fuse, does not co-localise with dextran.
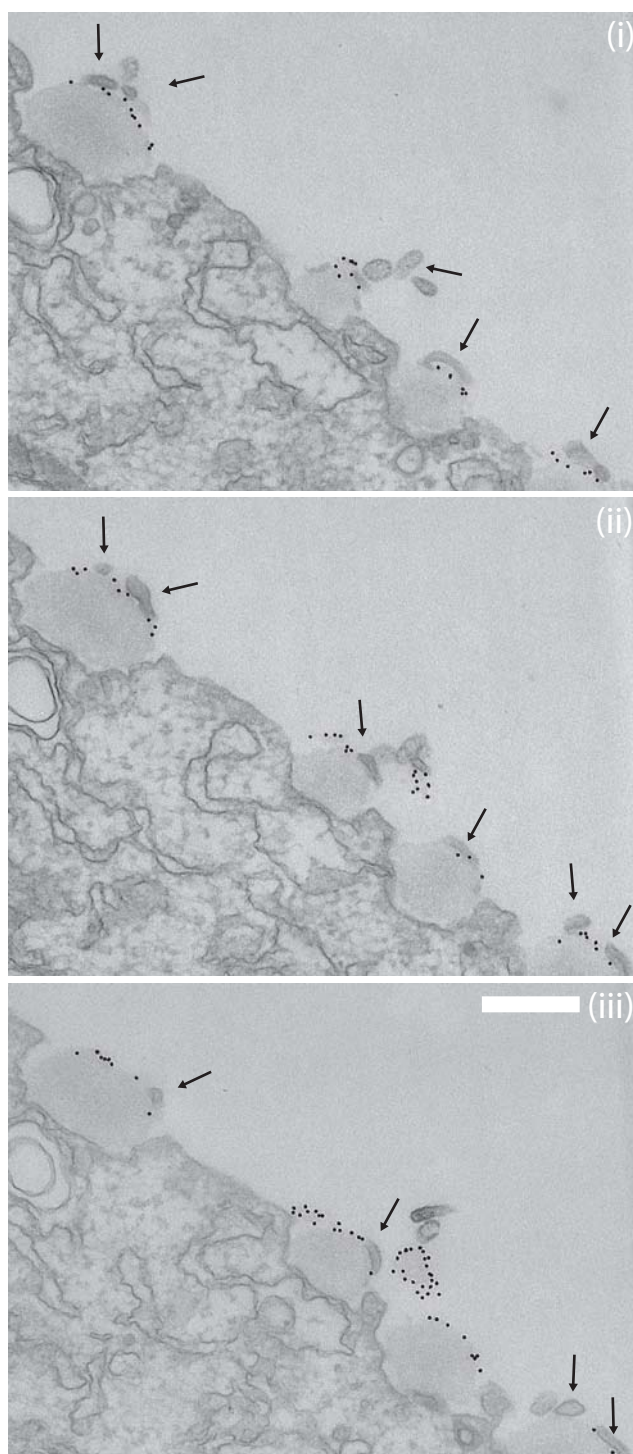
Figure S2. Multiple incomplete fusion events are apparent even in close proximity following actin depolymerisation

HUVEC were stimulated with PMA (100ng/ml) for 10 minutes in media supplemented with 1µM cytochalasin E (CCE). Cells were then fixed and external VWF labelled with anti-VWF antibodies before preparation for TEM. Serial sections are shown. Arrows show pieces of membrane still present around the fused exocytic structure, scale bar 500nm.
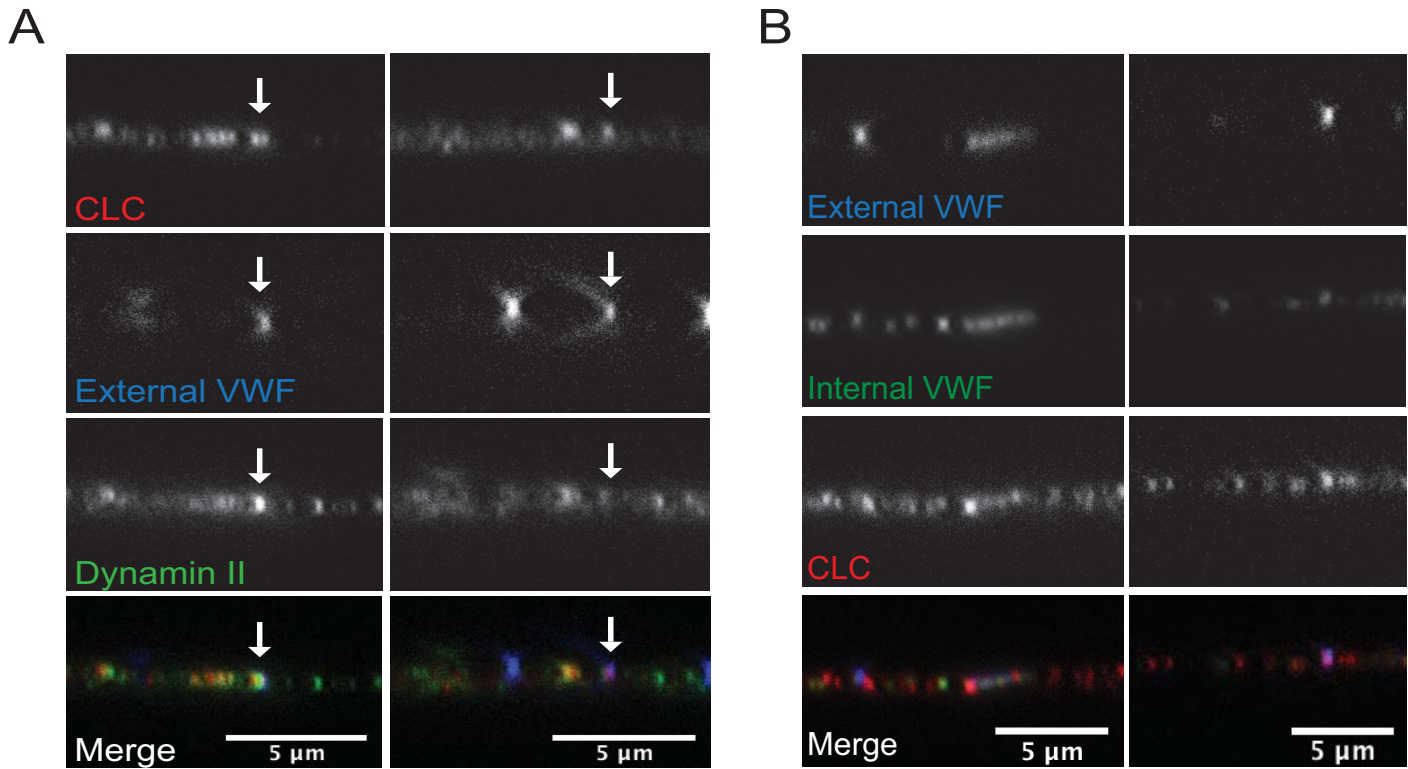
Figure S3. Clathrin and sometimes dynamin II co-localise with sites of string release

(A) Confluent HUVECs were stimulated with 100ng/ml PMA for 5 minutes at 37^0C then fixed and stained for external VWF (blue), dynamin II (green) and CLC (red). Cells were then imaged by confocal microscopy in the longitudinal plane to examine co-localisation between exocytosed VWF and clathrin at the exocytic pore. Single plane images are presented. Scale bar 5 µm. (B) Confluent HUVECs were stimulated with 100ng/ml PMA for 5 minutes at 37^0C then fixed and stained for external VWF (blue), total VWF (green) and CLC (red). Cells were then imaged by confocal microscopy in the longitudinal plane to examine co-localisation between exocytosed VWF and clathrin at the exocytic pore. Single plane images are presented. Scale bar 5 µm.
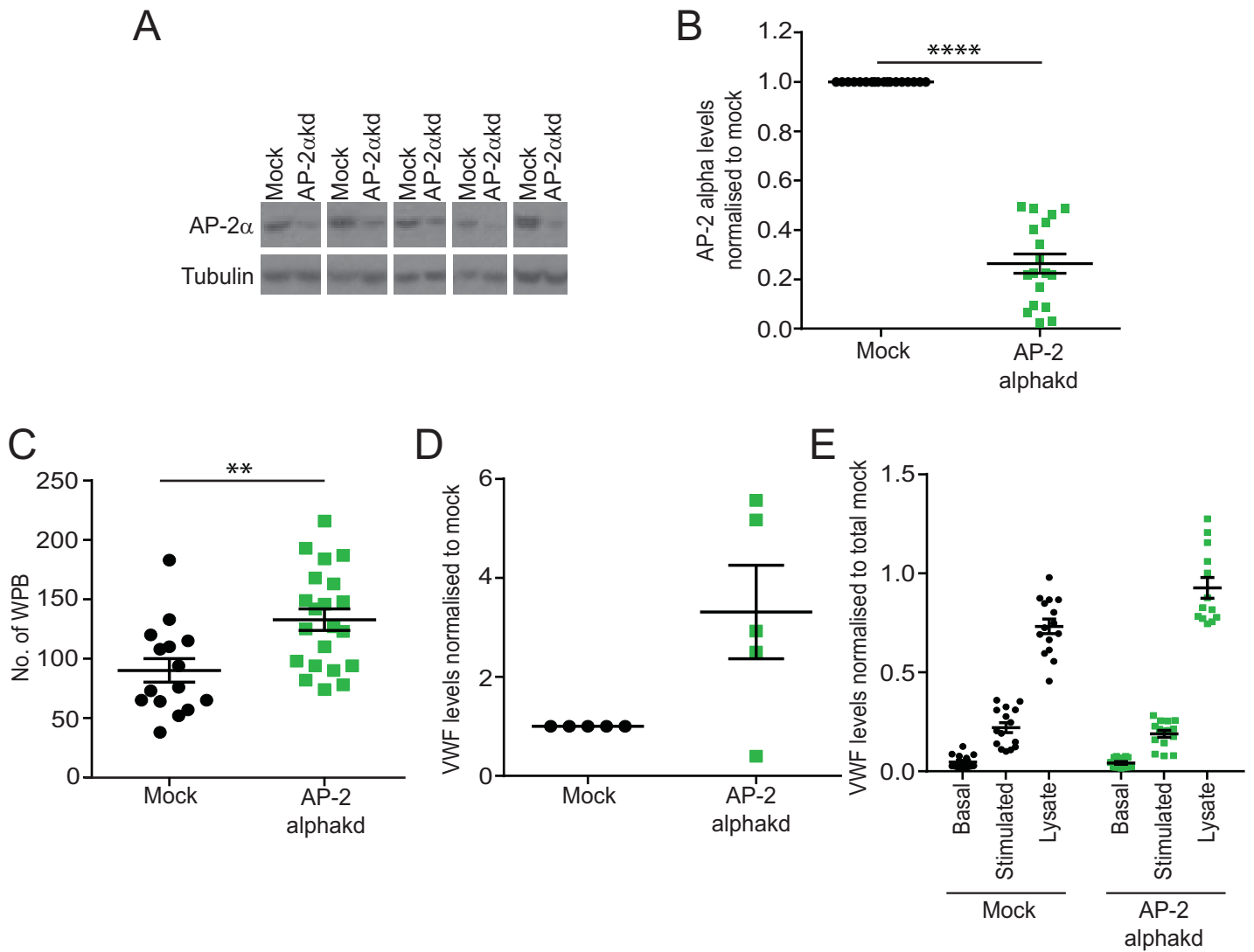
Figure S4. siRNA mediated knockdown of AP-2 alpha increases the number of WPB in endothelial cells.

(A-E) HUVEC were transfected with 300 pmol siRNA targeting AP-2 alpha for one or two rounds. (A & B) The extent of kd was determined by SDS PAGE and western blot. (A) Examples of western blots from 5 separate experiments showing AP-2 kd vs. the loading control β-tubulin. (B) Quantification of kd normalised to β-tubulin and relative to the mock, kd efficiency was on average 74% over 19

experiments. Error bars show SEM and statistics shown derived from unpaired student's T test on raw data (P=<0.0001). (C) At the second round of AP-2 alpha kd transfection 5μg GFP-VWF was incorporated and the cells were imaged live on a scanning confocal microscope. Images were taken and the number of WPB determined using Fiji and an arbitrary threshold. The number of WPB following AP-2 alpha kd was significantly increased. Error bars show SEM and statistics shown derived from unpaired student's T test (P=<0.005) n=5 experiments. (D) Quantification of VWF levels normalised to β-tubulin and relative to the mock, error bars show SEM n=5 experiments. (E) VWF levels as determined by ELISA. The amount of unreleased VWF in lysates was higher in AP-2 alpha kd cells compared to mock treated controls, error bars show SEM for n=5 experiments.

Table S1 – Co-localisation between internalised fluid-phase HRP and other proteins

SD = standard deviation. Data is the mean of 8-12 fields of view

Marker		Unstimulated cells	Stimulated cells	Student's t-test
EEA1	tM1	0.182 (SD = 0.046)	0.161 (SD = 0.038)	P = 0.285
	tM2	0.166 (SD = 0.038)	0.147 (SD = 0.063)	P = 0.278
P-selectin	tM1	0.195 (SD = 0.137)	0.207 (SD = 0.091)	P = 0.745
	tM2	0.03 (SD = 0.054)	0.111 (SD = 0.068)	P = 0.000063 ***
Transferrin	tM1	0.162 (SD = 0.037)	0.117 (SD = 0.117)	P = 0.421
	tM2	0.162 (SD = 0.030)	0.175 (SD = 0.063)	P = 0.261